T H E U N I V E R S I T Y O F T U L S A

THE GRADUATE SCHOOL

A PRIORI CHARACTERIZATION OF LOCALITY WITHIN SEQUENTIAL-IMPLICIT NONLINEAR SOLUTION PROCESSES

by
Soham M. Sheth

A thesis submitted in partial fulfillment of
the requirements for the degree of Master of Science
in the Discipline of Petroleum engineering

The Graduate School
The University of Tulsa

2014

T H E U N I V E R S I T Y O F T U L S A

THE GRADUATE SCHOOL

A PRIORI CHARACTERIZATION OF LOCALITY WITHIN SEQUENTIAL-IMPLICIT NONLINEAR SOLUTION PROCESSES

by
Soham M. Sheth

A THESIS

APPROVED FOR THE DISCIPLINE OF

PETROLEUM ENGINEERING

By Thesis Committee

_____, Advisor
Rami M. Younis

_____
Mohan Kelkar

_____
Randy Hazlett

ABSTRACT

Soham M. Sheth (Master of Science in Petroleum engineering)

A Priori Characterization of Locality within Sequential-Implicit Nonlinear Solution Processes

Directed by Rami M. Younis

73 pp., Chapter 5: Discussion

(266 words)

Flow in porous media is characterized by a set of coupled nonlinear governing equations, arising due to the volume averaging process of the continuum. These equations invariably exhibit a localized character in space and time. Transport variables, exhibiting a hyperbolic wave nature, evolve very locally while flow variables, essentially parabolic waves, show a relatively global support. Characterizing the nonzero support of the change in the state variables holds immense application. Many heuristic methods have been developed to exploit this knowledge of locality in the past, but little to no work has been done on deriving analytic formulations. Moreover, it is hypothesized that certain closed form analytical models that depend solely on known parameters of the system provide a *priori* characterizations of the support. This thesis aims at characterizing the spatiotemporal evolution of the multiscale flow and transport systems analytically.

This approach first proceeds by forming the fully-implicit, semi-discrete in time, set of equations. This is followed by obtaining the infinite-dimensional Newton iterations, solutions of which result in the updated state variables. In this, each iterate is the solution of a linear, steady state Partial Differential Equation; the solution itself is the Newton update. The sum of these updates is the instantaneous change in the state variables over the time step.

The practical implications of this work are far-reaching; uncertainty quantification and simulation model developers will know the precise locality of any dynamic multiphase

displacement before knowing its complete state. This can lead to the development of numerical techniques in multiscale numerical simulation of oil and gas recovery that perform on orders of magnitude more computationally efficiently.

ACKNOWLEDGEMENTS

This is the toughest part of concluding my work. There are at least a million people I would like to acknowledge, who helped me throughout my master's degree. I thank you for your unconditional support throughout.

First and foremost I would like to thank Dr. Rami M. Younis for accompanying me on this journey and not just being a great guiding light but a friend as well. I would also like to thank Dr. Mohammad Shahvali for his counsel throughout my studies and my committee members, Dr. Mohan Kelkar and Dr. Randy Hazlett for their valuable input and encouragement. I would also like to thank Dr. Albert Reynolds for his excellent teaching and insight into the courses which served as the platform for my learning.

An important part of these two years in and out of the office were my friends and team mates at FuRSST. I thank Ruslan Miftakhov, Walter Poquioma, Jiang Jiamin and Shahriyar AlKhasli (and all those whose names I couldn't write) for your continuous support and help at every step. Without the administrative staff, I would not have gone far. I take this moment to specially thank Loreta Watkins for her spotless management and administrative skills. s I am most thankful to my parents ,Monishi and Namita Sheth, for their constant support and guidance throughout the journey of life. I also thank my Fiancé, Heena Sisodiya, for trying her best not to distract me and keeping me on the right track.

And finally, I would like to thank people at The University of Tulsa's Board for providing me with the opportunity to be a teaching assistant and fund my study.

TABLE OF CONTENTS

LIST OF FIGURES

CHAPTER 1

INTRODUCTION

Petroleum recovery processes invariably couple physical phenomena that are characterized by a disparate range of spatiotemporal scales [6, 29]. A first-order source of such coupling is within the constitutive relations for flow in porous media that arise through the volume averaging process of continuum modeling. One specific example of this is the coupling between pressure and saturation *via* the multiphase extension to Darcy's law [33]. Physical systems that involve such character are referred to as *multiscale* systems. Another source of coupling across scales arises in petroleum recovery processes due to the fact that the overall integrated process will often involve multiple types of physics. For example, geomechanics and multiphase flow are coupled to well-bore flow [36]. Such systems are referred to as *multiphysics* systems. This thesis seeks to further our understanding of the spatiotemporal evolution of multiscale and multiphysics systems that are broadly central to petroleum recovery systems. The proposed approach is analytical, and it is restricted to the focal setting of petroleum recovery systems that are modeled by a certain canonical form. This canonical form is introduced mathematically later in this section. The canonical form encompasses the general governing equations for transient multiphase multicomponent flows in heterogeneous porous media with the possibility for chemical reactions and coupling to advanced well-bore flows.

Multiscale and multiphysics coupling is invariably accompanied by an inherent, and dynamically evolving, spatiotemporal locality. While one set of physics evolves globally, other phenomena exhibit a relatively local evolution. There is further complexity in such physical systems; the transitions across characteristic regimes, and the scale separations across various coupled subprocesses are often nonlinear and state dependent. Subsequently,

the precise nature of the spatiotemporal locality in the evolution of state variables is difficult to characterize. In general heterogeneous and nonlinear settings, analytical models of such systems are limited, and numerical simulation is necessary for the purposes of modeling for prediction and assessment [4, 12].

The numerical simulation of multiscale and multiphysics systems is fundamentally challenged by a curse of dimensionality. Specifically, in numerical simulation, the space-time domain is discretized and approximations of the state variables at discrete points or elements are sought. The *resolution* of the discrete domain refers to level of granularity of the discretization, whereas the *extent* of the domain refers to its overall size. The dimensionality of the discrete domain is the product of the resolution and the extent. In multiscale and multiphysics systems, the global physics will dictate the extent of the discrete spatial and temporal domain while the local physics will dictate its resolution. The wider the gap between the global and local characteristic scales, the larger is the dimensionality of the full-resolution discrete system. Both globally and locally evolving state variables need to be solved under the same imposed dimension of the discrete domain. This implies that the computational complexity of such simulations is far greater than the intensity of change in the physical variables.

This leads to a timely topic of research in the design of numerical simulation methods. Modern advances in the simulation of such phenomena aim to take advantage of the spatiotemporal locality of the evolution of certain state variables in order to reduce the necessary computational effort [20]. Ideally, and especially in light of the geometric growth in the complexity of emerging applications, this is accomplished with an amount of computation that is directly proportional to the amount of change in state variables. Next we review methods in Numerical Simulation that strive to exploit locality in one form or another.

1.1 Methods that exploit locality

Modern simulation methods for complex nonlinear multiscale problems overwhelmingly follow the Adaptive Discretization paradigm. In this paradigm, the numerical approxi-

mation itself is adaptively modified in space, time, or both in order to improve the method's computational efficiency. In doing so, while the objective of adaptive computation is often achieved, the integrity of the approximation's accuracy and robustness may be compromised or require additional effort for it to be maintained.

One example of a promising Adaptive Discretization method is Adaptive Mesh Refinement or Dynamic Gridding [9, 21, 40, 19]. In these methods, the spatial discretization of the domain is dynamically altered by refining its resolution in locales where changes in state are occurring locally and by coarsening the resolution elsewhere. This class of method is particularly effective for homogeneous problems that evolve with a predominant travelling-wave character. Under heterogeneity, homogenization strategies are necessary every time the mesh is adapted [19]. This leads to additional computational expense, and more importantly, to additional approximation errors associated with the homogenization process. For problems that have components which evolve with a more global character, the efficacy of Adaptive Mesh Refinement methods is relatively limited. Advances in the identification of locality can help mitigate some of the concerns surrounding the use of AMR.

Another promising Adaptive Discretization method is the use of a spatially varying temporal discretization [18, 16]. These methods are also referred to as local time-stepping or adaptive time-step refinement methods [31, 34]. In this class of method, parts of the domain where a state variable is experiencing rapid change, the numerical integration is performed using a fine temporal resolution compared to other locales. While such methods are proving to be effective for hyperbolic problems that involve sharp frontal advancement, there are potentially serious challenges to their application for parabolic problems with more global character. In particular, for such problems, synchronization strategies are required in order to inform neighboring locales of the locally occurring rapid changes in state. Reliable *a priori* knowledge of any locality that may be present could lead to a class of local timestepping methods that are effective even for parabolic problems. In such schemes, there would be no need for any synchronization despite the parabolic character.

Adaptive Multiscale methods are an alternate form of Adaptive Discretization strat-

egy that do not rely on the dynamic adaptation of the discrete domain [1, 24, 25, 32]. Rather, in this approach, the state variables that evolve on a more global scale are integrated using coarsened representations. These representations are tied to the remaining state variables that are represented by fine scale equations.

An emerging alternate paradigm to the Adaptive Discretization class of method is the Adaptive Solver approach. In the Adaptive Solver approach, the key idea is to apply full-resolution, fully-coupled approximations that are static, and to innovate underlying solvers that are themselves dynamically adaptive to a varying spatiotemporal support. Since the numerical approximation itself is unmodified, there are no impending fidelity or accuracy concerns and these methods can in principle combine the efficiency of adaptive computation with the fidelity of well-established numerical approximations. Examples in this class of method include adaptive localization strategies [46] and solutions that exploit potential based orderings [28]. Another example is the development of adaptive nonlinear preconditioners that are based on domain decomposition ideas [11, 23]. These nonlinear solvers were recently applied to basic petroleum recovery applications [38, 37].

All of these adaptive numerical methods require the answer to one fundamental question. Given a particular instant in time, suppose that we are informed of the present dynamic and static states of the system that is under consideration. In what part of the spatial domain will the dynamic state experience change? This part of the domain is called the *support* as it supports nontrivial instantaneous changes in the state. What does the support depend on and how?

1.2 Associated work on the topic of locality

The character of the evolution of flow and transport state variables and of their associated spatial supports is complex. Moreover, as discussed in the previous section, an accurate characterization of this evolution is paramount for the future success and efficiency of simulation methods for emerging multiscale and multiphysics petroleum recovery processes. In the broadest context, the spatiotemporal locality of dynamic change continues to be a subject of

study [22], and in the more specific context of general multiphase flow and transport, there is still no fundamental and universally applicable characterization of it. In this section, we first review associated work on the topic. This is followed by a technical introduction to the proposed approach towards a fundamental and universally applicable characterization.

In the literature, there are two approaches to the study of locality and to the development of ways to exploit it in computation. The first approach is **indirect** and seeks to characterize locality through the study of the resulting approximation errors in models for the system. Classic examples of such work include the error estimate derivations [5, 43] and the reviews [2, 41], as well as several recent applications such as [35, 47, 14, 39]. These and other successful error-based adaptivity investigations and applications are well-established for the flow (Equation 1.4.2), transport (Equation 1.4.3), and coupled (Equation 1.4.1) problems.

The second approach towards characterizing and exploiting locality that is reported on in the literature is **direct**. Direct studies of locality in unrelated physical systems include the flow of traffic [42], which exhibits a traveling wave character, and accretive transport phenomena [30]. On the other hand, in studies that are focused on flow and transport phenomena, works following the direct approach are further categorized as either (a) those that tackle general systems while seeking to devise *ad hoc* characterizations, or (b) those that deal with limiting cases and idealized systems while seeking exact and analytical results. Examples of the former, are the sharp discontinuity detection procedures that are applicable to transport problems [8, 7, 10]. In these procedures, the focus is on the detection of fronts and in the application of linearized approximations and local Courant-Friedrichs-Lewy numbers to guess the support. Examples of the latter are studies regarding the notion of a *radius of investigation* in pressure transients about wells in flow problems [27, 44, 13]. In these studies, while idealizations are made regarding the limitation on the phases present and on the level and nature of the underlying homogeneity, the results are exact.

The motivation for the present work stems from a recent advance that was made at FuRSST(Future Reservoir Simulation Systems and Technology) [45]. In this advance, a direct approach is taken to the study of locality in decoupled flow and transport systems. The

approach tackles general flow and transport problems that incorporate general nonlinearity and heterogeneity in one-dimension. The study derives a sharp analytical bound that characterizes the spatiotemporal support of change for decoupled flow and transport systems. It achieves this by utilizing the infinite-dimensional Newton method [15], and it provides links to the discrete problem through recent developments in the derivation of an Asymptotic Mesh Independence Principle [3, 26].

This thesis will focus on a specific and yet broad setting for multiphase flow and transport. For this setting, a hypothesis regarding the character of the instantaneous spatiotemporal support is made. The proposed work makes conjectures of specific estimates for the size, location, and rate of growth of the support that depend on parameters that are already known. It is then proposed that an innovative analytical framework be applied in order to validate and analyze the hypothesized conjectures.

1.3 The computational kernel in simulation

Petroleum recovery processes are modeled by a set of nonlinear and inhomogeneous partial differential equations obtained by applying mass, momentum and energy balance concept on a continuum. These equations, for the case of isothermal flow, are obtained by the combination of the conservation of mass with Darcy's law [33]. The nonlinear coupling between elliptical flow and hyperbolic transport equation introduces further complexity in the system. Conservation of mass for a two-phase flow system can be described by Equation 1.3.1.

$$\frac{\partial(\rho_\alpha \phi S_\alpha)}{\partial t} + \nabla\left(\rho_\alpha \vec{v}_\alpha\right) = g_\alpha, \tag{1.3.1}$$

where, g_α is the phase volumetric sink/source term and v_α is the superficial phase velocity given by the multiphase extension of Darcy's law

$$\vec{v}_\alpha = -\frac{\overline{\overline{K}} k_{r\alpha}}{\mu_\alpha}\left(\nabla p_\alpha - \rho_\alpha g\right), \tag{1.3.2}$$

where $\overline{\overline{K}}$ is the heterogeneous permeability tensor and $\frac{k_{r\alpha}}{\mu_\alpha}$ is the phase mobility designated

by λ_α. Capillary pressure is a nonlinear function of saturation and is formulated as the difference in pressures of the non-wetting phase to the wetting phase, $p_c = p_{non} - p_{wet}$.

Mathematically, reservoir simulation can be described as a technique to obtain the solution of a set of equations given by Equation 1.3.1. Due to the heterogeneous and complex nature of the equations, analytical solutions are limited and only possible to certain simplified and homogeneous problems. In order to obtain the solution for a complex case, numerical simulation techniques must be adopted. In this, the continuous partial differential equations are discretized in space and time, leading to a discrete continuum. The discretization in time can be treated explicitly or implicitly. Explicit scheme evaluates the constitutive nonlinear functions at the old state reducing the number of unknowns to one, which can be directly evaluated by simply substitution. In spite of being a computationally efficient scheme, it is restricted by stability. On the other hand, the implicit scheme evaluates the functions at the current state, which introduces a number of unknowns. To solve this system of equations a simultaneous solution method must be employed. This scheme has unconditional stability but at the price of computational efficiency. In this thesis we will focus on the fully implicit scheme for the time discretization. Each grid block in the discrete continuum has its independent governing equation and a state. As opposed to the continuous problem, in the discrete domain, each sub continuum has homogeneous properties while preserving nonlinear dependencies and complex character of the governing equation. Owing to the nonlinear characteristics of the equations, iterative numerical methods can be employed to solve for the state variables. One of the most extensively used fixed-point iteration schemes as the computational kernel is the Newton's method.

Newton's iterations follow a gradient based paradigm. At each iteration it generates an update function which is the solution to a linear system of equations. To obtain the consecutive updates, computation of the derivative of the function with respect to every state is required. In the discrete simulation case, the residual function, or the governing equation, is a vector of equations for the discrete continuum. Consequently, the derivative generated is a matrix called the Jacobian given by

$$\begin{bmatrix} \frac{\partial \mathcal{R}_1}{\partial u_1} & \frac{\partial \mathcal{R}_1}{\partial u_2} & . & . & . \\ \frac{\partial \mathcal{R}_2}{\partial u_1} & \frac{\partial \mathcal{R}_2}{\partial u_2} & . & . & . \\ . & . & \frac{\partial \mathcal{R}_3}{\partial u_3} & . & . \\ . & . & . & . & . \\ . & . & . & . & \frac{\partial \mathcal{R}_n}{\partial u_n} \end{bmatrix};$$

The product of residual vector ($\mathcal{R}$) to the inverse of the Jacobian matrix ($\mathbf{J}$) gives the update which when added to the old state generates the new set of state variables. Starting from the initial state, also knows as the initial guess, the scheme iteratively converges to the solution. Equation 1.3.3 gives one such iteration step with the initial guess , $\left[\vec{U}^1\right]^{\nu=0} = \vec{U}^0$.

$$\left[\vec{U}^{n+1}\right]^{\nu+1} - \left[\vec{U}^{n+1}\right]^{\nu} = -\mathbf{J}^{-1}\mathcal{R}\left(U^{n+1}; U^n, \Delta t\right); \tag{1.3.3}$$

1.4 Formal objectives and proposed approach

The physical system this thesis covers is concerned with the evolution of two sets of independent state variables - flow and transport. Flow, exhibiting a parabolic wave nature, evolves locally at very early times but in sometime its effect can felt at the reservoir boundaries. There variables are denoted by $p(\vec{x}, t)$, where $\vec{x} \in \mathbb{R}^3$ is the position vector and $t \geq 0$ is the temporal variable. Pressure attains steady state and evolves in an elliptic manner exhibiting a global support in the change of state variables. On the other hand, transport variables, denoted by $s(\vec{x}, t)$, evolve locally exhibiting a hyperbolic wave character.

1.4.1 Examples of locality in flow and transport

Consider the case of 2 phase black oil model in multiple dimensions. The reservoir is described by the permeability tensor which has a heterogeneous distribution and the pressure independent porosity. The spatial domain is discretized using a 40 X 60 X 6 Cartesian grid. The problem modeled here consists of 2 phase flow (oil and water) with 2 injection wells and 5 production wells located throughout the domain. The well constraints are Bottom Hole Pressure (BHP) with injection pressure 5000 psi and production wells are operated at 800

psi. The initial pressure in the reservoir is determined by the gravity-capillary equilibrium. This system is modeled by the Equation 1.4.1 with specific expressions for the composite nonlinear terms which are flux, accumulation and the source.

Figure 1.1 shows the pressure distribution at time $t = 15$ days for a 2 dimensional slice containing the second layer. Evident from the figure, the support of the instantaneous change in the flow variable is global. The entire domain is contained in the Newton's nonzero update set. In other words, the update vector is a dense vector. In spite of this characteristic feature, it can be observed that some Newton's updates are significantly greater in magnitude than the rest i.e. locally around the wells. Hence, it can be concluded that there is some degree of locality present even in the case of a global update function.

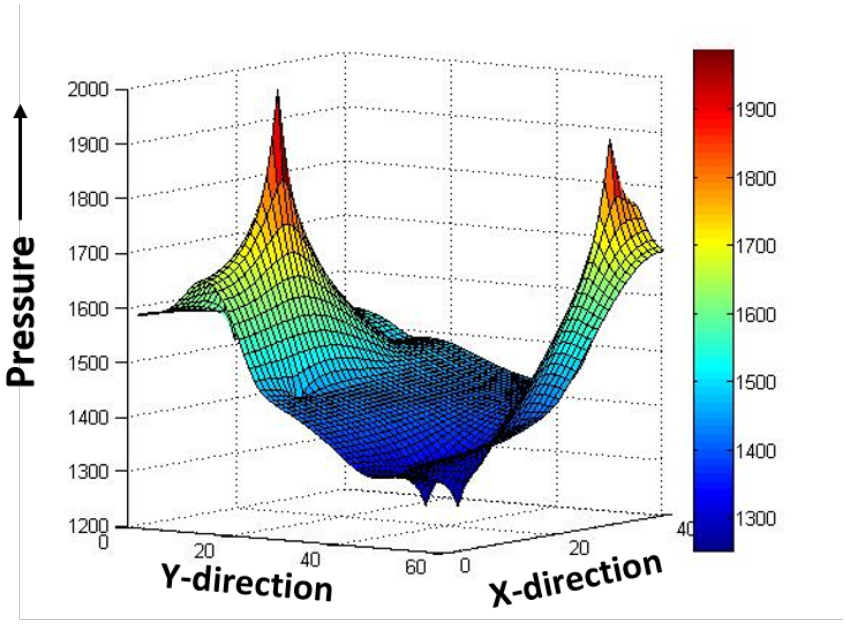

Figure 1.1: Pressure distribution along a 2 dimensional slice in a 3 dimensional problem. The global support of the flow variables dictate the reservoir boundaries.

On the other hand, Figure 1.2 depicts the saturation distribution after a simulation of 1200 days in a 2 dimensional plane. Unlike the flow equation, transport evolves in a strictly local manner possessing a hyperbolic wave characteristic. The transport waves emanate from the wells and traverse towards the rest of the reservoir. The locality in the support of the instantaneous change is governed by the nonlinear wave dynamics as well as by the underling

heterogeneity. Unlike the pressure equation, saturation equation preserves the locality over a timescale of years.

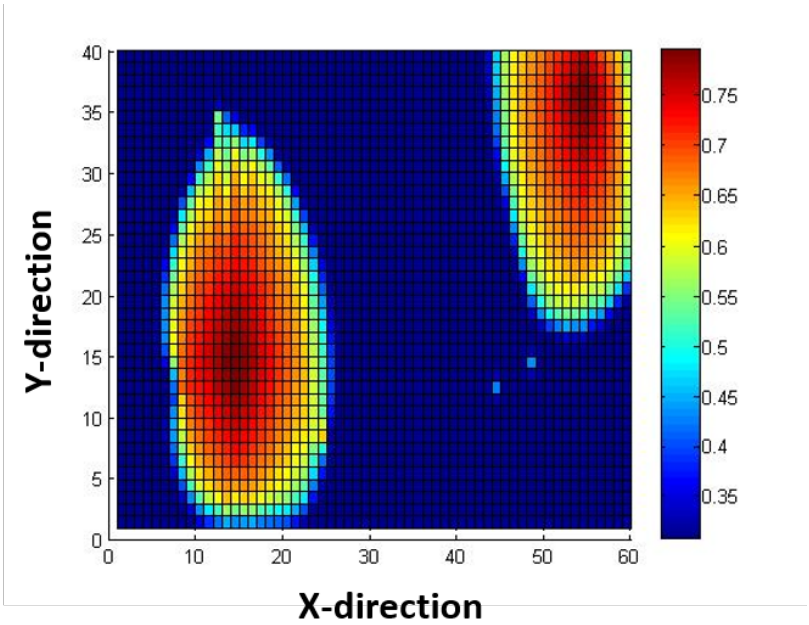

Figure 1.2: Saturation distribution along a 2 dimensional slice in a 3 dimensional problem. Local evolution of the hyperbolic transport equation can be seen.

1.4.2 The canonical form

The flow and transport state variables evolve according to a set of coupled governing equations given by Equation 1.3.1. This partial differential equation can be reduced to a canonical form wherein only the notation is simplified without hampering the complexity and nonlinearity. Throughout this thesis we will consider the canonical form, given by Equation 1.4.1 and establish connections to the numerical scheme.

$$\begin{cases} \mathcal{R}(p,s) = \frac{\partial}{\partial t} a(p,s) - \nabla\left[\mathbf{k}(p,s)\nabla p\right] + g(\vec{x},t) = 0 & \vec{x} \in D \subset \mathbb{R}^3,\ t \geq 0, \\ \mathbf{k}(p,s)\nabla p = 0, & \vec{x} \in \partial D,\ t \geq 0, \\ (p,s) = (p^0, s^0), & \vec{x} \in D,\ t = 0, \end{cases} \tag{1.4.1}$$

where $\mathcal{R}$ is the general nonlinear residual operator. The accumulation term, a, is generally

nonlinear and it incorporates a heterogeneous porosity and general density dependencies. The mobility function, $\mathbf{k}$, incorporates a spatially varying permeability tensor and a dynamic mobility dependency. The net source term is denoted as g, and it may be spatially and temporally variable. Finally, the auxiliary conditions in Equation 1.4.1 prescribe a no-flow outer boundary condition (Neumann boundary condition), which alternatively can be a constant pressure boundary (Dirichlet boundary condition), and a compatible initial condition.

The nonlinear functional terms, accumulation, mobility, and net sources, appearing in the governing equations are generally functions of both saturation and pressure. This fact leads to the nonlinear coupling between the flow and transport. One of the methods of obtaining an approximate solution to this coupled system is by sequentially isolating the pressure and transport components (see for example. [4]). This is accomplished by successively freezing the functional dependencies; for example $a(p, s)$ is considered as $a(p)$, with a frozen saturation state, s, that becomes a parameter rather than a variable. In one iteration of this strategy, transport is frozen and a decoupled pressure is obtained. The new pressure is subsequently frozen and an updated transport variable is obtained. The sequential strategy continues with such iterations until convergence.

The general form of the flow equation with frozen transport terms is given by Equation 1.4.2 with Neumann boundary conditions and initial reservoir conditions,

$$\begin{cases} \mathcal{R}_{\mathcal{F}}(p) = \frac{\partial}{\partial t} a(p) - \nabla\left[\mathbf{k}(p)\nabla p\right] + w(\vec{x}, t) = 0 & \vec{x} \in D \subset \mathbb{R}^3,\ t \geq 0, \\ \mathbf{k}(p)\nabla p = 0, & \vec{x} \in \partial D,\ t \geq 0, \\ p = p^0, & \vec{x} \in D,\ t = 0, \end{cases} \tag{1.4.2}$$

The transport equation, on the other hand, is

$$\begin{cases} \mathcal{R}_{\mathcal{T}}(s) = \frac{\partial}{\partial t} a(s) - \nabla . \mathbf{f}(s) + w(\vec{x}, t) = 0 & \vec{x} \in D \subset \mathbb{R}^3,\ t \geq 0, \\ \mathbf{f}(s) . \hat{\mathbf{n}} = 0, & \vec{x} \in \partial D,\ t \geq 0, \\ s = s^0, & \vec{x} \in D,\ t = 0, \end{cases} \tag{1.4.3}$$

Here, $\mathbf{f}$(s) is the dimensionless fractional flow function which describes fraction of the total flow that consists of the wetting phase. This quantity depends on the dynamic phase mobilities which essentially depend on the relative permeabilities being a nonlinear function of saturation.

1.4.3 The basic question

Consider the dynamic flow problem given by Figure 1.3, where the current state, U^n, is a static snapshot of the state variable at some arbitrary time $t \geq 0$. The updated state, U^{n+1}, after a small increment in time is obtained by computing the local Newton updates for the global system and adding the nonzero updates to the old state.

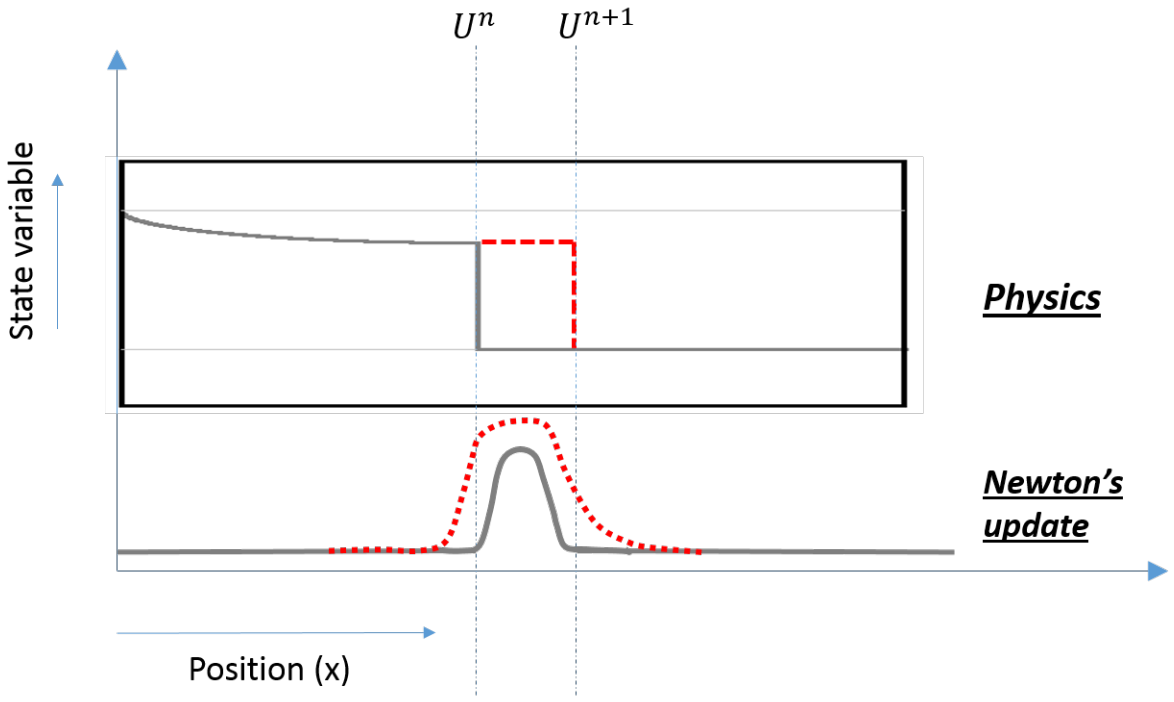

Figure 1.3: Instantaneous change in the state variable over a small increment in time, δt, and the corresponding nonzero Newton update.

In the systems that are described by one of the canonical forms given by Equations 1.4.1 through 1.4.3, what will be the instantaneous spatiotemporal support in the change in the flow and transport variables over a given time-step Δt, and what parameters does it depend on? This questions has to be answered for any heterogeneous and complex system, independent of the choice of underlying spatial discretization.

Mathematically, at any given instant in time, $t \geq 0$, suppose that we are provided with the knowledge of the current states of the system; $p(x \in D, t)$ and $s(x \in D, t)$. We are interested in the support of change in the state variables over an infinitesimal time increment, $\delta t \geq 0$. Analytically, instantaneous change in the flow over this time increment is given by

$$\delta_p = \|p\,(x, t + \delta t) - p\,(x, t)\|\,,$$

which may be expressed in transport variable as

$$\delta_s = \|s\,(x, t + \delta t) - s\,(x, t)\|$$

In Figure 1.3 this instantaneous change in the state variables is described by the rectangular area confined between the states, U^n and U^{n+1}. In terms of Newton's method, it is given by the nonzero update, solid line, as shown in the lower half of the figure. We are seeking to characterize the set of point that are incorporated in the compact spatiotemporal support for the change in flow,

$$\Omega_p = supp\,(\delta_p)\,,$$

and in transport variables,

$$\Omega_s = supp\,(\delta_s)\,.$$

In Figure 1.3 this conservative estimate is given by the dashed curve in the Newton update (lower half of the figure). The Equations 1.4.1 are time dependent and generally highly nonlinear partial differential equations that are coupled through flow and transport inducing a hybrid hyperbolic-elliptic character. Previous work on these equations suggest that obtain-

ing an analytical solution for the general canonical case [17] is next to impossible. Hence, instead of searching for the solution of the equation, it may be more analytically tractable to derive a sharp and conservative estimate $\hat{\delta}_{p,s}$ such that

$$\hat{\delta}_{p,s} \geq \delta_{p,s} \geq 0$$

and subsequently we would obtain a conservative estimate of the support in the actual change in state variable set since

$$\Omega_{p,s} \subseteq \tilde{\Omega}_{p,s} = supp\left(\hat{\delta}_{p,s}\right);$$

To characterize the support or the estimate of support, the canonical equation must be solved analytically. There is no analytical solution for a general full form canonical equation. There are solutions which make assumptions and reduce the set of equations into simplified ones. The definitive determination of the support, $\Omega_{p,s,}$, or the estimate of support, $\tilde{\Omega}_{p,s,}$, hold major applications.

1.4.4 Proposed approach: Analytical overview

The proposed approach takes the analytical route which aims at determining a *priori* conservative estimate of the support, i.e. $\tilde{\Omega}_{p,s}$. The aim is to obtain a sharp universal estimate which is independent of the underlying spatial discretization. This section introduces the procedure to derive the abstract Newton's iterations, and further on, case specific solutions are provided.

In this thesis we will study the evolution of the state analytically. Instead of a vector of states in the numerical simulation, here we will study state as a function of space and time, given by

$$U\left(\vec{x},t\right) : \Omega \subseteq \mathbb{R}^N$$

Considering a general equation governing flow and transport systems described by

$$\mathcal{R}(U) = \frac{\partial a(U)}{\partial t} + \mathcal{F}(U, \nabla U, \Delta U)$$

and compatible boundary and initial conditions. The task here is to deduce the spatiotemporal support of the instantaneous change in the state variables over a small time step, Δt. The instantaneous change is given by

$$\delta_{\Delta t} = U(\vec{x}, t + \Delta t) - U(\vec{x}, t).$$

The first step to characterize this change is to look for the solution of the equation formed by the Newton's iteration. The possibility of obtaining an analytical solution to the general form is next to impossible. Hence, we go about by semi discretizing the equation in time resulting in a partial differential equation continuous in space. The semi discrete form is

$$\mathcal{R}\left(U^{n+1}\right) = a\left(U^{n+1}\right) - a\left(U^{n}\right) + \Delta t \mathcal{F}\left(U^{n+1}, \nabla U^{n+1}, \Delta U^{n+1}\right) \tag{1.4.4}$$

In flow and transport systems, this equation is highly nonlinear and complex. Hence, to find a solution, Newton's method is used which translates the problem to a linear differential equation given by Equation B.0.5.

$$\mathcal{R}\left(\left[U^{n+1}\right]^{\nu}\right) = \mathcal{R}'\left(\left[U^{n+1}\right]^{\nu}\right)\left(\left[U^{n+1}\right]^{\nu+1} - \left[U^{n+1}\right]^{\nu}\right), \tag{1.4.5}$$

where

$$\left[U^{n+1}\right]^{\nu+1} - \left[U^{n+1}\right]^{\nu} = \delta^{\nu+1};\ \nu = 0, 1, 2...,\ n = 0, 1, 2...$$

which generates the Newton iterates. This flavor of Newton's method is characterized as a continuous fixed point iteration schemes, known as infinite dimensional Newton's method [15]. Unlike the discrete or scalar Newton's method, here we treat the residual equation as a nonlinear partial differential equation. For more information on infinite dimensional Newton's method, refer Appendix B.

In Equation B.0.5, $\mathcal{R}$ is the nonlinear residual operator and is a functional(refer to appendix A) of space and time. The derivative of a functional is computed using the Frećhet derivative(refer Appendix A), which is the derivative of the residual equation that is evaluated at the current iterate, $[U^{n+1}]^{\nu}$, and applied onto the Newton update, $\delta^{\nu+1}$. The Frećhet derivative is given by

$$\mathcal{R}'\left(\left[U^{n+1}\right]^{\nu}\right)\delta^{\nu+1} = \lim_{\epsilon\to 0}\frac{\mathcal{R}\left(\left[U^{n+1}\right]^{\nu}+\epsilon\delta^{\nu+1}\right)-\mathcal{R}\left(\left[U^{n+1}\right]^{\nu}\right)}{\epsilon}; \tag{1.4.6}$$

The derivation of Equation 1.4.6 is also referred to as *quasilinearization* as it generates an operator that is nonlinear in the state but linear in the current Newton update, $\delta^{\nu+1}$. For the functional forms of partial differential equations that we are focused on, Equation B.0.5 is invariably of the form

$$f\left(\mathbf{x}\right)\Delta\delta^{\nu+1} + g\left(\mathbf{x}\right)\nabla\delta^{\nu+1} + h\left(\mathbf{x}\right)\delta^{\nu+1} = -\mathcal{R}\left(\left[U^{n+1}\right]^{\nu}\right), \tag{1.4.7}$$

where the variables coefficients *f, g* and *h* are general functions of the current Newton's iterate, $[U^{n+1}]^{(\nu)}(\mathbf{x})$, and its spatial derivatives. The coefficients have a variable behavior due to the underlying heterogeneity that is present in the governing partial differential equation. Equation 1.4.7 is linear in the unknown Newton update, δ^{v+1}, and can be solved at each iteration, $\nu = 0, 1, 2, ...$, to generate the sequence of Newton updates analytically.

1.4.5 Solution strategies for the infinite dimensional Newton iteration

Unlike the discrete Newton's method, where a linear system of equation is solved to obtain the unknown update, a partial differential equation must be solved at each Newton step. This equation is described by Equation 1.4.7 where f,g, and h are functions of the update and space. Due to the variable nature of the coefficients, a closed form analytical solution for the Newton's iteration may not be possible. In the solution of large-scale algebraic linear systems, often indirect and preconditioned methods are used to obtain estimates of the Newton updates. Similarly, instead of solving Equation 1.4.7, we will solve for a

conservative, and yet sharp, estimate for the Newton update, $\hat{\delta}^{(\nu)}$ such that it satisfies

$$\left|\hat{\delta}^{(\nu)}\right| \geq \left|\delta^{(\nu)}\right|; \tag{1.4.8}$$

Consequently, an upper bound to the nonzero support of the change in the state variables can be computed, since

$$supp\left(\hat{\delta}^{(\nu)}\right) \supseteq supp\left(\delta^{(\nu)}\right) \tag{1.4.9}$$

The strategies adopted in this thesis to obtain the estimates that satisfy Equation 1.4.8 can be divided into two groups. The first group deals with the analytical homogenization of the variable coefficients appearing in Equation 1.4.7 on a global scale. The second group deals with the exploitation of the principle of superposition and homogenizing the variables on a local scale. The second group can be loosely related to the domain decomposition methods.

The analytical homogenization of the variable coefficients within the Frećhet derivative can be as simple as taking the supremum or infimum of the coefficients, such as

$$f^* = \sup_{\mathbf{x}\in\Omega} f\left(\mathbf{x}\right);$$

There can be many different homogenization techniques that can be used to recast the linear differential equation into a form which has constant coefficients. Equation 1.4.10 shows the differential equation linear in the Newton update with constant coefficients.

$$f^*\Delta\hat{\delta}^{\nu+1} + g^*\nabla\hat{\delta}^{\nu+1} + h^*\hat{\delta}^{\nu+1} = -\mathcal{R}\left(\left[U^{n+1}\right]^{\nu}\right) \tag{1.4.10}$$

With a careful choice of the homogenization strategy, a conservative and sharp estimate to the actual Newton update can be obtained.

Next is introduced a strategy which will prove useful in cases of disjoint local domains. This exploits the linearity inherent to the problem and principle of superposition. The

residual can be written as the sum of k bump functions,$\phi_i(\mathbf{x})$ where $i = 1, 2, ...k$. Each of these bump functions have disjoint compact support, $supp(\phi_i(\mathbf{x})) = D_i \subseteq \Omega$, i.e. $D_i \cap D_j = \emptyset$ where $i \neq j$. Residual as the summation of the bump functions is given by,

$$\mathcal{R}\left(\left[U^{n+1}\right]^{\nu}\right) = \sum_{i=1}^{k} \phi_i(\mathbf{x})$$

Substituting this definition of the residual operator, Equation 1.4.10 can represented as,

$$f^* \sum_{i=1}^{k} \Delta\hat{\delta}_i^{\nu+1} + g^* \sum_{i=1}^{k} \nabla\hat{\delta}_i^{\nu+1} + h^* \sum_{i=1}^{k} \hat{\delta}_i^{\nu+1} = -\sum_{i=1}^{k} \phi_i(\mathbf{x}) \tag{1.4.11}$$

The Newton update is obtained by,

$$\hat{\delta}^{\nu+1} = \sum_{i=1}^{k} \hat{\delta}_i^{\nu+1}$$

This strategy is very important in situations where the support of the residual consists of the union of a collection of strongly connected components.

CHAPTER 2

THE FLOW EQUATION

Among the two sets of variables, flow evolves in an parabolic/elliptic fashion. In the early times around the wells, the pressure variables show a local support, exhibiting a parabolic wave nature. In a short time, the pressure waves reach the reservoir boundary, showing relatively global support. At steady state, pressure shows elliptic wave characteristics.

In this section we will derive the analytical estimate of the Newton update for the flow problem. First, we will deduce a general Frećhet derivative of the decoupled canonical flow equation given by Equation 1.4.2. Secondly, we will find the estimate of the solution for the *quasilinear* infinite dimensional Newton iteration described by a linear differential equation in the unknown update.

2.1 Infinite dimensional Newton iterations

The canonical form for the decoupled flow equation is given by,

$$\mathcal{R}_{\mathcal{F}}(p) = \frac{\partial}{\partial t} a(p) - \nabla\left[\mathbf{K}(p)\nabla p\right] + w(\vec{x}, t) = 0 \tag{2.1.1a}$$

where $\vec{x} \in D \subset \mathbb{R}^3,\ t \geq 0$ and boundary and initial conditions as,

$$\mathbf{K}(p)\nabla p = 0 \qquad \mathbf{x} \in \partial D,\ t \geq 0, \tag{2.1.1b}$$

$$p = p^0 \qquad \mathbf{x} \in D,\ t = 0 \tag{2.1.1c}$$

Here, the boundary condition is described as a Neumann condition which is a no flow boundary. Instead of this condition, a Dirichlet condition might be considered in cases where there

is a constant pressure boundary maintained by an aquifer.

Towards the solution of Equation 2.1.1a, with auxiliary conditions given by Equation 2.1.1b and 2.1.1c, the first step is deriving the semi-discrete form, maintaining continuity in space. Applying the backward Euler discretization in time to Equation 2.1.1a, we obtain,

$$\begin{cases} \mathcal{R}_{\mathcal{F}}(p^{n+1}) = \mathbf{a}(p^{n+1}) - \mathbf{a}(p^n) - \Delta_t \nabla[\mathbf{K}(p^{n+1})\nabla p^{n+1}] + \Delta_t w(x,t) = 0 & \mathbf{x} \in D \subset \mathbb{R}^3,\ t \geq 0, \\ \mathbf{K}(p^{n+1})\nabla p^{n+1} = 0 & \mathbf{x} \in \partial D,\ t \geq 0, \\ p^{n=0} = p_{init}\,(x) & \mathbf{x} \in D \subset \mathbb{R}^3,\ t = 0 \end{cases} \tag{2.1.2}$$

$n = 0, 1, 2 \ldots$

As stated in the previous sections, Newton iteration produces the sequence of functions,

$$\left[p^{n+1}\right]^{\nu+1} - \left[p^{n+1}\right]^{\nu} = \delta^{\nu+1};\ \nu = 0, 1, 2 \ldots,\ n = 0, 1, 2 \ldots$$

where, $\delta^{\nu+1}$ is the Newton update and is obtained as the solution to a linear differential equation. Just to save some writing efforts, $p^{(\nu)}$ is equivalent to $[p^{n+1}]^{\nu}$ from this point onwards.

After transforming the general canonical form to the semi-discrete equation, we will derive the Frećhet derivative for Equation 2.1.2. This step gives us a linear differential equation with respect to the unknown update but still preserves the nonlinearity with respect to space.

The first step towards deriving a Frećhet derivative is to add a perturbation in the functional by an infinitesimal scalar quantity in the direction of the unknown update, $\delta^{(\nu+1)}$. We are looking for the gradient between the current flow state variables and the perturbed state, given by,

$$p^{(\nu)} + \epsilon\delta^{(\nu+1)}$$

The residual equation has to be evaluated at this perturbed state. This results in the perturbed form of Equation 2.1.2,

$$\mathcal{R}_{\mathcal{F}}(p^{\nu}+\epsilon\delta^{\nu+1}) = \mathbf{a}([p^{n}]^{\nu})-\mathbf{a}(p^{\nu}+\epsilon\delta^{\nu+1})-\Delta_{t}\nabla[\mathbf{K}(p^{\nu}+\epsilon\delta^{\nu+1})\nabla\left(p^{\nu}+\epsilon\delta^{\nu+1}\right)]+\Delta_{t}w(p^{\nu}+\epsilon\delta^{\nu+1}) = 0 \tag{2.1.3}$$

Frećhet derivative is obtained using Equation 2.1.4,

$$\mathcal{R}'_{\mathcal{F}}\left(p^{\nu}\right)\delta^{\nu+1} = \lim_{\epsilon\to 0}\frac{\mathcal{R}\left(p^{\nu}+\epsilon\delta^{\nu+1}\right)-\mathcal{R}\left(p^{\nu}\right)}{\epsilon} \tag{2.1.4}$$

and the result is given by,

$$\mathcal{R}'_{\mathcal{F}}\left(p^{\nu}\right)\delta^{\nu+1} = \left[a'\left(p^{\nu}\right)+\Delta_{t}w'\left(p^{\nu}\right)\right]\delta^{\nu+1}-\Delta_{t}\Delta\left(\mathbf{K}\left(p^{\nu}\right)\delta^{\nu+1}\right)-\nabla\left(\frac{\partial\mathbf{K}\left(p^{\nu}\right)}{\partial x}\delta^{\nu+1}\right) \tag{2.1.5}$$

where, $\nu = 0, 1, \ldots$. In the above equation, Δ represents the Laplacian operator which is given by the divergence of the gradient, $\nabla\cdot\nabla$. Equation 2.1.5 is the *quasilinear* differential equation with respect to the unknown Newton update. We can further reduce this equation by making proper substitutions, provided, $\Delta_{t}\mathbf{K}\left(p^{\nu}\right) \neq 0$. We can simplify the Frećhet derivative by introducing a new variable,

$$\hat{\delta}^{\nu+1} = \Delta_{t}\mathbf{K}\left(p^{\nu}\right)\delta^{\nu+1}$$

Equation 2.1.5 becomes,

$$\mathcal{R}'_{\mathcal{F}}\left(p^{\nu}\right)\delta^{\nu+1} = \left[\frac{a'\left(p^{\nu}\right)+\Delta_{t}w'\left(p^{\nu}\right)}{\Delta_{t}\mathbf{K}\left(p^{\nu}\right)}\right]\hat{\delta}^{\nu+1}-\Delta\hat{\delta}^{\nu+1}-\nabla\left(\frac{1}{\Delta_{t}\mathbf{K}\left(p^{\nu}\right)}\frac{\partial\mathbf{K}\left(p^{\nu}\right)}{\partial x}\hat{\delta}^{\nu+1}\right) \tag{2.1.6}$$

The infinite dimensional Newton iteration can be formulated now and is given by,

$$\begin{cases} \Delta\hat{\delta}^{\nu+1} - h\left(x\right)\hat{\delta}^{\nu+1} + \nabla\left(\frac{1}{\Delta_t \mathbf{K}(p^{\nu})}\frac{\partial \mathbf{K}(p^{\nu})}{\partial x}\hat{\delta}^{\nu+1}\right) = \mathcal{R}_{\mathcal{F}}\left(p^{\nu}\right) & x \in D \\ \nabla\hat{\delta}^{\nu+1}_{x=\partial D} = 0, \end{cases}, \ \nu = 0, 1, \ldots \tag{2.1.7}$$

where,

$$h\left(x\right) = \frac{a'\left(p^{\nu}\right) + \Delta_t w'\left(p^{\nu}\right)}{\Delta_t \mathbf{k}\left(p^{\nu}\right)}$$

and $\mathcal{R}_{\mathcal{F}}\left(p^{\nu}\right)$ is the nonlinear residual equation.In theabove equation,

$$\nabla\left(\frac{1}{\Delta_t \mathbf{K}\left(p^{\nu}\right)}\frac{\partial \mathbf{K}\left(p^{\nu}\right)}{\partial x}\hat{\delta}^{\nu+1}\right)$$

is the term which accounts for the spatial variation of permeability. The gradient of permeability with respect to the space variables is different for a heterogeneous case while for a homogeneous case, goes to zero. For the present derivation, we will consider the gradient of permeability to be zero and then try and consider the application of this estimate to the heterogeneous case.

Equation 2.1.7 must be solved analytically to obtain a closed form solution of the update. Since this equation is highly heterogeneous and complex, a closed form solution may not be possible. As our strategy describes, we seek a conservative estimate to the actual Newton update. For this purpose we employ a homogenization strategy which removes the heterogeneity from the equation ensuring a conservative upper bound to the actual Newton update. The objective of this step is to homogenize the coefficient $h(x)$ in order to obtain a simplified equation of the form,

$$\Delta {\delta_*}^{\nu+1} - h^* {\delta_*}^{\nu+1} = \mathcal{R}_{\mathcal{F}}\left(p^{\nu}\right) \tag{2.1.8}$$

where,

$$|{\delta_*}^{\nu+1}| \geq |\hat{\delta}^{\nu+1}| = |\Delta_t \mathbf{K}\left(p^{\nu}\right)\delta^{\nu+1}| \tag{2.1.9}$$

First, we note that depending on the sign of h^*, the linear homogenized equation is either in the form of a screened Poisson equation ($h^* \geq 0$) or a Helmholtz equation ($h^* < 0$). In the case of screened Poisson equation, one of the homogenization strategies that is adopted in this thesis is taking the largest value of the screening coefficient over the domain. The homogenization that ensures a conservative estimate is

$$h^* = \sup_{x \in D} h(x);$$

On the other hand, the Helmholtz equation produces Newton updates that are oscillatory where the coefficient h^* is the wave number or frequency. In the petroleum applications, $h(x)$ is always positive, and hence, we will assume the first case. Finally, the homogenized linear Newton update problem becomes

$$\begin{cases} \Delta {\delta_*}^{\nu+1} - \lambda^2 {\delta_*}^{\nu+1} = \mathcal{R}_{\mathcal{F}}\left(p^{\nu}\right) \quad x \in D \\ \nabla {\delta_*}^{\nu+1}_{x=\partial D} = 0, \end{cases}, \ \nu = 0, 1, \ldots \tag{2.1.10}$$

where

$$\lambda = \sqrt{h^*};$$

Equation 2.1.10 describes the general Newton iteration, which must be now solved for the sharp but conservative estimate, ${\delta_*}^{\nu+1}$.

2.2 Analytical solution

To get the analytical closed form solution of the general canonical form is impossible because of the heterogeneous and variable coefficients. Hence, we reduced the equation by applying the infinite dimensional Newton concept to a linear differential equation which can be solved for a conservative estimate of the actual update. Now we can solve Equation 2.1.10 using different analytical solution methods. The degree of dimensions govern the boundary conditions and in some case free form analytical solutions on infinite domains. For this reason, we will derive the solution for specific dimensions.

Figure 2.1 describes the problem setting for the one dimensional case. The boundaries are at $x = 0$, the origin, and $x = 1$, the right boundary. Every problem can be normalized into this scenario. The source term in our case is a production/injection well with appropriate well constraints.

The one dimensional homogenized linear Newton update problem with Neumann boundary conditions is given by,

$$\begin{cases} \frac{\partial^2}{\partial x^2}{\delta_*}^{\nu+1} - \lambda^2 {\delta_*}^{\nu+1} = \mathcal{R}_{\mathcal{F}}\left(p^{\nu}\right) \quad x \in [0,1]\,, \\ \left[\frac{\partial}{\partial x}{\delta_*}^{\nu+1}\right]_{x=0} = 0, \qquad\qquad\qquad\qquad , \ \nu = 0,1,\ldots \\ \left[\frac{\partial}{\partial x}{\delta_*}^{\nu+1}\right]_{x=1} = 0, \end{cases} \tag{2.2.1}$$

where,

$$\lambda = \sqrt{h^*}.$$

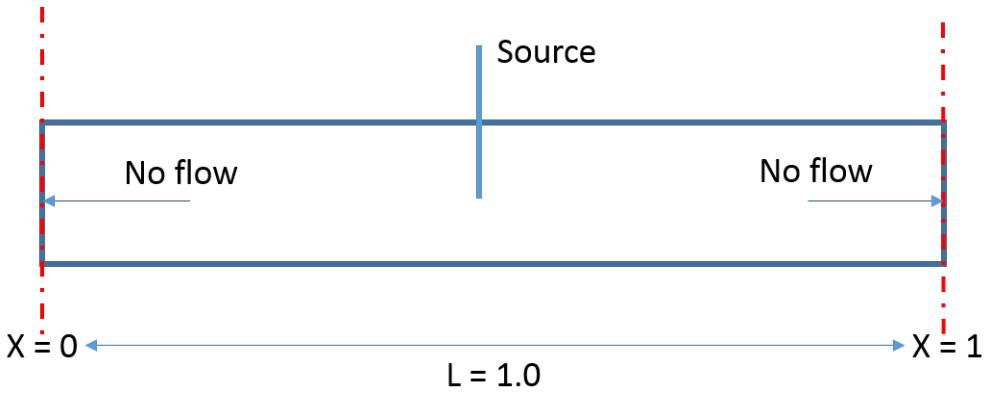

Figure 2.1: One dimensional problem statement with no-flow reservoir boundaries.

Considering the form of Equation 2.2.1, Greens functions can be used to look for a solution. The fundamental solution to,

$$\frac{\partial^2}{\partial y^2}\Phi\left(x-y\right) - \lambda^2\Phi\left(x-y\right) = \delta\left(x-y\right),$$

in the sense of distributions is well known. It is,

$$\Phi(x-y) = -\frac{1}{2\lambda}\exp(-\lambda|x-y|).$$

Subsequently, if we can find a corrector function, $l(y;x)$, satisfying,

$$\begin{cases} \frac{\partial^2}{\partial y^2} l(y;x) - \lambda^2 l(y;x) = 0, & y \in [0,1] \\ \left[\frac{\partial}{\partial y} l(y;x)\right]_{y=0} = \left[\frac{\partial}{\partial y}\Phi(x-y)\right]_{y=0}, \\ \left[\frac{\partial}{\partial y} l(y;x)\right]_{y=1} = \left[\frac{\partial}{\partial y}\Phi(x-y)\right]_{y=1}, \end{cases} \tag{2.2.2}$$

then we can define the Green's function,

$$G(x,y) = \Phi(x-y) - l(y;x),$$

which produces the solution to Equation 2.2.1 in the form,

$$\delta_*{}^{\nu+1} = \int_0^1 G(x,y)\,\mathcal{R}_{\mathcal{F}}(p^{\nu}(y))dy. \tag{2.2.3}$$

In order to solve Equation 2.2.2, we will first write out the Neumann boundary conditions, in other words, evaluating the fundamental solution at the boundaries. Noting that the investigation point is always in the domain, $x \in [0,1]$, we have,

$$\left[\frac{\partial}{\partial y} l(y;x)\right]_{y=0} = -\frac{1}{2}e^{-\lambda x},$$

and,

$$\left[\frac{\partial}{\partial y} l(y;x)\right]_{y=1} = \frac{1}{2}e^{-\lambda(1-x)}.$$

Subsequently, we obtain the corrector function, $l(y;x)$, as,

$$l(y;x) = \frac{1}{\lambda(e^{2\lambda}-1)}\left[\cosh(\lambda x)\,e^{\lambda y} + e^{\lambda}\cosh(\lambda(x-1))e^{-\lambda y}\right],$$

and the associated Green's function becomes,

$$G(x,y) = \frac{1}{\lambda}\begin{cases} [\sinh(\lambda x) - \mu\cosh(\lambda x)]\cosh(\lambda y) & \text{if } x \geq y \\ \cosh(\lambda x)[\sinh(\lambda y) - \mu\cosh(\lambda y)] & \text{if } x < y \end{cases}, \tag{2.2.4}$$

where,

$$\mu = \frac{e^{2\lambda}+1}{e^{2\lambda}-1}.$$

Once we have the solution for the homogeneous equation, we can couple the inhomogeneous term with the Green's function. This step deals with the decomposition of the right-hand-side, $\mathcal{R}_{\mathcal{F}}(p^{\nu}(y))$, into the sum of $k \geq 0$ bump functions. We are concerned with the effects of a nontrivial residual, $\mathcal{R}_{\mathcal{F}}(p^{\nu}(y)) \neq 0$, for $y \in [0,1]$. Suppose that the residual consists of the sum of $k \geq 1$ bump functions,

$$\mathcal{R}_{\mathcal{F}}(p^{\nu}(y)) = \sum_{i=1}^{k} \phi_i(y),$$

each of which is supported over a connected interval,

$$D_i = \operatorname{supp}(\phi_i) = \left[L_a^i, L_b^i\right] \subseteq \Omega.$$

Moreover, we can assume that the intervals are mutually disjoint; $D_i \cap D_j = \emptyset$, for $i \neq j$. Hence, for points within the nonzero support, $y \in \cup_{i=1}^{k} D_i$, the residual is nonzero, and otherwise, it is zero. Finally, we can homogenize each of the constituent bump functions independently. In particular, let the stationary point, y^*, be defined as,

$$y^* = \arg\max_{y \in D_i} |\phi_i(y)|,$$

and its corresponding value as,

$$\phi_i^* = \phi_i(y^*).$$

Then the homogenized form of the bump function is simply,

$$\phi_i^*(y) = \begin{cases} \phi_i^* & y \in D_i \\ 0 & y \in \Omega - D_i \end{cases}.$$

Finally, the Newton update is obtained as the superposition of solutions,

$$\begin{aligned} {\delta_*}^{\nu+1} &= \sum_{i=1}^{k} {\delta_*}_i^{\nu+1} \\ &= \sum_{i=1}^{k} \phi_i^* \int_{L_a^i}^{L_b^i} G(x,y) dy. \end{aligned}$$

The last step includes the solution of the linear Newton updates to compute the estimate. For the i-th bump function, we can obtain a corresponding Newton update component by integrating the Green's function (Equation 2.2.4). Because the Green's function is defined piecewise, we need to perform the integral for various situations.

First we will assume that the support of the given right hand side, D_i, is a single point; i.e., $L_a^i = L_b^i = L_*$. In this case, the bump function is a delta distribution, $\phi_i^* \delta(y - L_*)$. The update in this case is simply,

$$\begin{aligned} {\delta_*}^{\nu+1} &= \phi_i^* \int_0^1 G(x,y)\, \delta(y - L_*) dy \\ &= \phi_i^* G(x; L_*). \end{aligned}$$

The analytical formula for the estimate to the update is therefore,

$$\delta_{*,i}^{\nu+1} \approx \frac{\phi_i^*}{\Delta t k(p^\nu)} \frac{1}{\lambda} \begin{cases} [\sinh(\lambda x) - \mu \cosh(\lambda x)] \cosh(\lambda L_*) & \text{if } x \geq L_* \\ \cosh(\lambda x) [\sinh(\lambda L_*) - \mu \cosh(\lambda L_*)] & \text{if } x < L_* \end{cases}. \tag{2.2.5}$$

Next, we will consider cases where the right hand side function has a nontrivial support; $0 \leq L_a^i < L_b^i \leq 1$. In this situation the Green's function integral must be performed

assuming three cases; the first assumes that $x \leq L_a^i$, the second assumes that $L_a^i \leq x \leq L_b^i$, and finally , the third that $L_b^i \leq x$. The result is,

$$\delta_{*,i}^{\nu+1} \approx \frac{\phi_i^*}{\Delta t k\left(p^\nu\right)} \frac{1}{\lambda^2} \begin{cases} C_1 \left[\sinh\left(\lambda x\right) - \mu \cosh\left(\lambda x\right)\right] & \text{if } x > L_b^i \\ 1 + \left[\cosh\left(\lambda L_b^i\right) - \mu C_1\right] \cosh\left(\lambda x\right) - \sinh\left(\lambda L_a^i\right) \sinh\left(\lambda x\right) & \text{if } x \left[L_a^i, L_b^i\right], \\ \left[C_2 - \mu C_1\right] \cosh\left(\lambda x\right) & \text{if } x < L_a^i \end{cases} \tag{2.2.6}$$

where,

$$C_1 = \sinh\left(\lambda L_b^i\right) - \sinh\left(\lambda L_a^i\right),$$

and,

$$C_2 = \cosh\left(\lambda L_b^i\right) - \cosh\left(\lambda L_a^i\right).$$

2.3 Connection to numerical simulation

The analytical deduction of the support of the instantaneous changes in the state is connected to the discrete counterpart in numerical simulation. Specially, the infinite dimensional and finite dimensional results are connected through the accuracy of the numerical approximation. Consider a discrete domain, Ω_h, with the discrete state variables $U^n : \Omega_h \subseteq \mathbb{R}^N \to \mathbb{R}^N$. The finite-dimensional approximation to Equation 1.4.4 is the fully discrete residual system,

$$R_h\left(U^{n+1}\right) = A_h\left(U^{n+1}\right) - A_h\left(U^n\right) + \Delta t F_h\left(U^{n+1}\right) = 0, \tag{2.3.1}$$

where for some order of approximation, $p \geq 1$, and with appropriate norms, $\|\cdot\|$, the error is formally bounded as,

$$\left\|U^{n+1} - u^n\left(\mathbf{x}\right)\right\| = \mathcal{O}_1\left(h^p\right).$$

Newton's method applied to Equation 2.3.1 is written as,

$$J_h\left(\left[U^{n+1}\right]^{(\nu)}\right) \Delta^{\nu+1} = -R_h\left(\left[U^{n+1}\right]^{(\nu)}\right), \tag{2.3.2}$$

where J_h is the Jacobian matrix and the discrete Newton update is defined according to,

$$\left[U^{n+1}\right]^{\nu+1} - \left[U^{n+1}\right]^{\nu} = \Delta^{\nu+1}.$$

It is stated without proof that the fully discrete Newton update, Δ^{ν}, and the infinite-dimensional update, $\delta^{\nu}(\mathbf{x})$, are also related by the approximation accuracy;

$$\|\Delta^{\nu} - \delta^{\nu}(\mathbf{x})\| = \mathcal{O}_2\left(h^p\right).$$

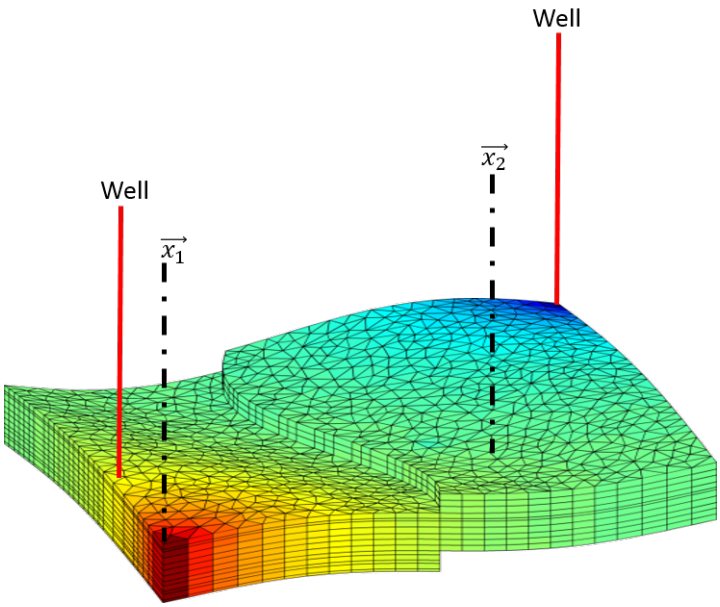

Figure 2.2: Discrete continuum representing the numerical problem. Taken from the MATLAB Reservoir Simulation Toolbox (MRST).

Figure 2.2 shows a hypothetical scenario where the analytical solution has to be correlated to the numerical. Given the grid information, i.e. the position vectors or in numerical words, grid block, source data and domain dimensions, we can evaluate the estimate of the Newton update at any point in the domain. Using this information directly into the analytical formulas derived in the prior sections will give us a quick estimation of the spatiotemporal change in the state variables across the numerical simulation domain. This holds many applications which will be discussed in the following chapters.

2.4 Results and conclusions

The aim here is to obtain an estimation of the support of the actual instantaneous change in the state variables, for a given time step, Δt. The results are obtained for decoupled flow for one dimensional problems. Complications lie in the algorithm to create the connection between the analytical results developed with the numerical simulation algorithm. Comparison between the numerical update to the estimation obtained from the solution of the analytical equations must result in a conservative estimate such that the support of the numerical update is contained in the support of the analytical estimate,

$$supp\left(\hat{\delta}^{(\nu)}\right) \supseteq supp\left(\delta^{(\nu)}\right)$$

One point to note is the analytical solution changes with the boundary conditions. The partial differential equation remains the same but the values of the variable constants change according to the nature of the boundary conditions. With the Neumann boundary condition the boundaries are no-flow while with Dirichlet condition, pressure remains constant at the boundaries. The first problem to be considered is a one dimensional flow problem with no-flow boundary conditions. The domain is highly heterogeneous and the nonlinearity in the functional terms is preserved. There is a source term at the center of the domain in the form of a bottom hole pressure controlled well. On applying the analytical formula derived, we obtain the green curve which is irregular in nature. This irregularity in the graph and the lack of smoothness is due to the homogenization of the variables coefficients encountered in the canonical equation. The blue curve which exhibits a smoothness in the curve is the numerical update obtained from the one dimensional pressure simulation for a certain time step, Δt.

The aim here was to obtain a conservative estimate of the actual instantaneous change in the state variables. In other words, support of the analytical solution must be a superset to the support of the numerical update.

To prove this point, any grid cell undergoing a nonzero Newton update is given the

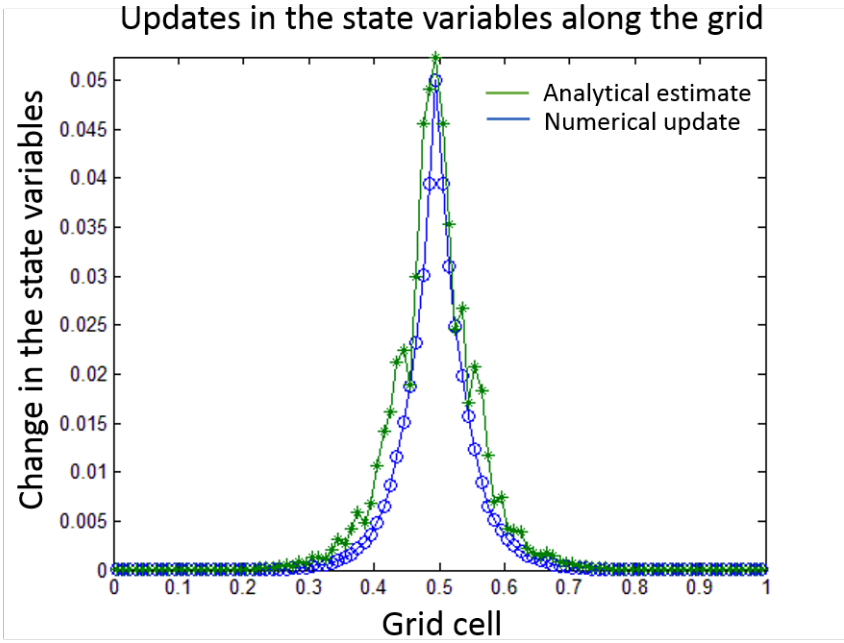

Figure 2.3: Comparison between the analytical, green curve, and the numerical update, blue curve, in the flow variables for one Newton solve.

value 1 while the cells with no instantaneous change are represented by 0. Figure 2.4 shows the same for analytical and the numerical solution obtained. The cells exhibiting a change in the state variables are represented by the line with a constant value of 1.0 while the rest is null. In figure 2.4, the green curve represents the support of the analytical estimate and the blue is the numerical update, wherein the estimate overshoots the support by a few grid cells. This ensures that the instantaneous change is contained in the estimated support for that particular time step.

It is claimed that for a heterogeneous case, irregularity in the curve for the analytical estimate is due to the homogenization step. Hence, if the case possessed homogeneous permeability field, the curve should be smooth and be an exact match to the numerical solution. Figure 2.5 gives the comparison between the analytical and numerical solutions for the instantaneous change in flow variables. Being a homogeneous case, the smoothness in the solution is evident from the figure. Green curve which represents the analytical solution is smooth and exactly traces the numerical solution as expected.

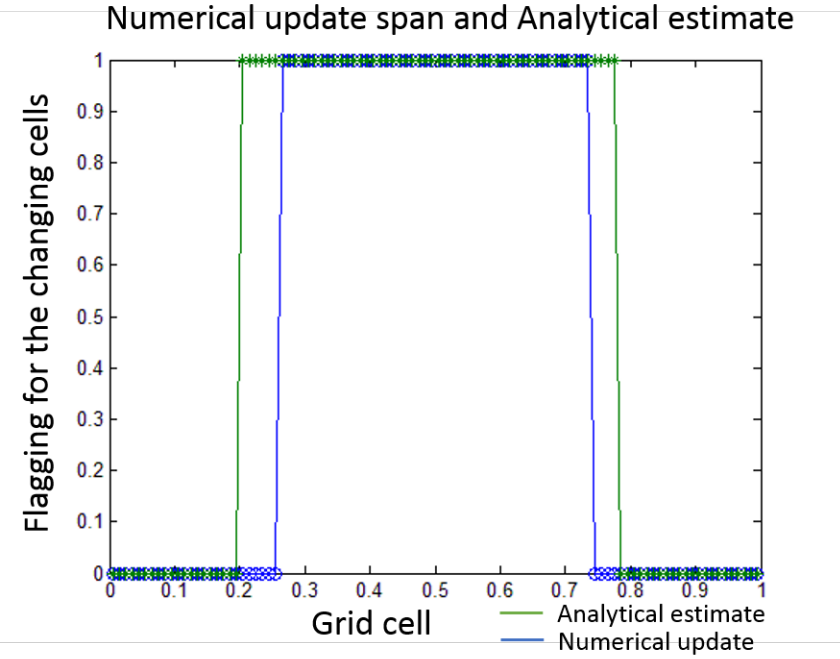

Figure 2.4: Support of the analytical estimate is a superset to support of the numerical update. Nonzero change in the state variable is given the value 1.0, otherwise it is 0.

To confidently state that the solution for a homogeneous case is almost exact, we will flag the cells with nonzero change and compare both the solutions. Figure 2.5 shows the same, which proves that the cells which are predicted to show a nonzero Newton update exactly match the ones obtained from the numerical simulation.

Next, we studied the formulation of a single nonzero residual source. In other words, the nonzero residual is transmitted to multiple cells from a single point. The situation is different and much more complicated when there are multiple nonzero residual sources.
To observe the behavior of the analytical solution for more complex scenarios, multiple sink and source terms are introduced by plugging in wells at different grid locations. Figure 2.6 shows the solution for multiple wells and comparison with the numerical update solution. It can be easily observed that the analytical solution is a conservative estimate of the actual newton update.

For a multiple well case, the comparison between the analytical and numerical solutions can be seen in Figure 2.7. The irregular plot on the right is due to the homogenization

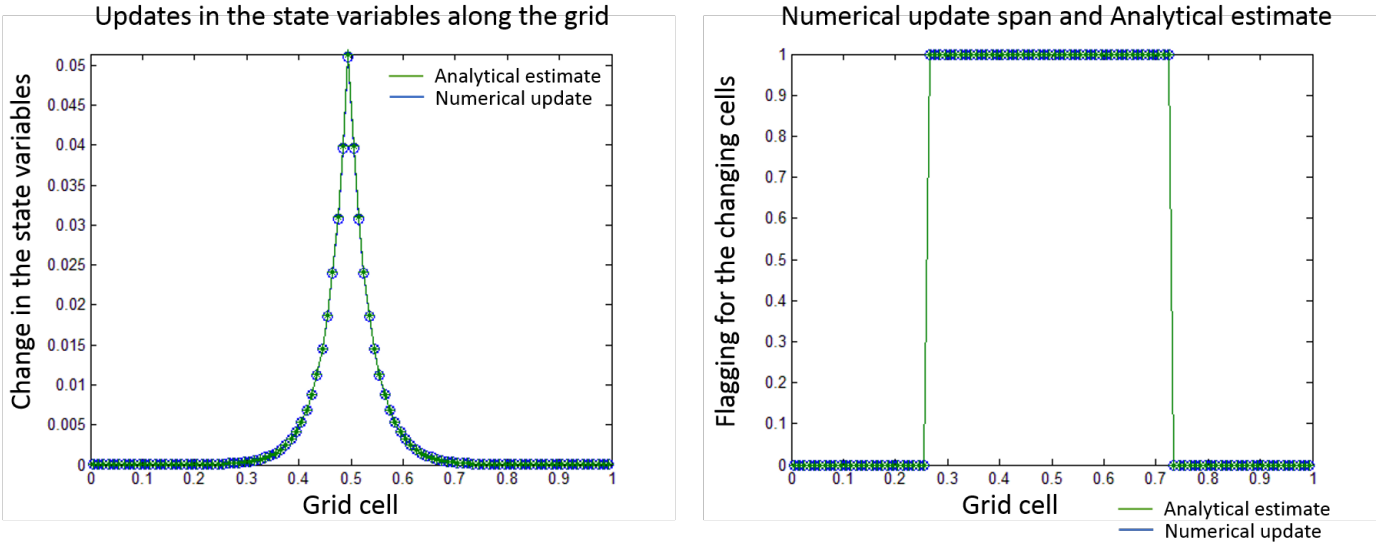

Figure 2.5: Comparison between the analytical and numerical solution for the Newton update for a homogeneous test case with a single point nonzero residual source. The support of analytical and numerical solution match exactly.

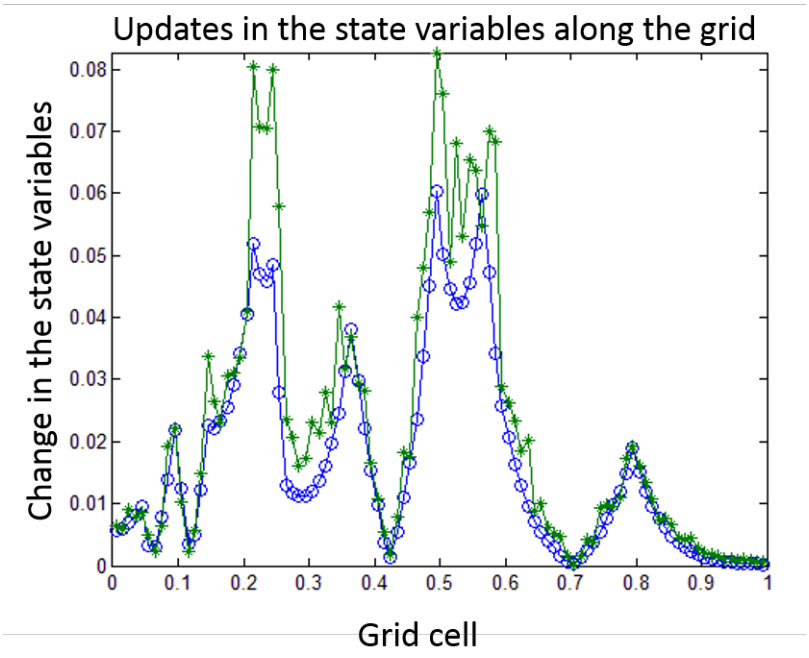

Figure 2.6: Multiple nonzero residual sources which increase the complexity of the problem. The analytical solution adapts to the inherent complex physics.

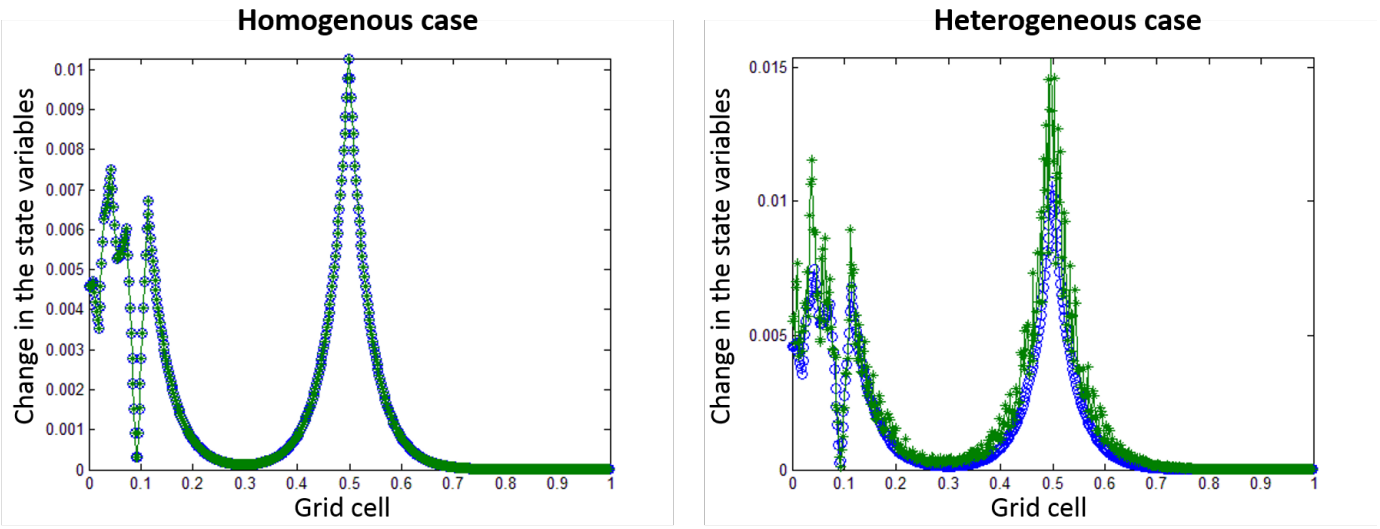

Figure 2.7: Comparison between the homogeneous and heterogeneous problem for multiple nonzero residual sources.

of the variable coefficients as discussed earlier in the sections.

An important test which must be performed is to refine the mesh to a greater degree and observe the behavior of the absolute error in the analytical to the numerical solution. One of the applications of the prediction of the instantaneous change in the variables is in developing novel nonlinear solvers which allow a very refined grid throughout the domain and adapt the computational kernel to the underlying spatiotemporal change. Figure 2.8 shows the relation between the resolution of the spatial discretization to the absolute error in the estimate of the Newton update. As expected, as the resolution increases, i.e. the mesh become finer the error decreases. The comparison is done between of 100, 500 and 5000 grid cells. It can be observed that the error decreases from 10^{-2} to the order of 10^{-4} when the grid size is changed from 100 to 5000 grid cells. This behavior is due to a better homogenization in finer grids than coarse. If we employ a very complicated homogenization strategy it is speculated that this error can be further decreased. To support this fact, we give the results for a homogeneous case and compare the error for the same problem with a heterogeneous permeability. Figure 2.9 shows the same and it can be confirmed that in the case where the homogenization is close to ideal, the error is in the order of 10^{-9} whereas for its heterogeneous

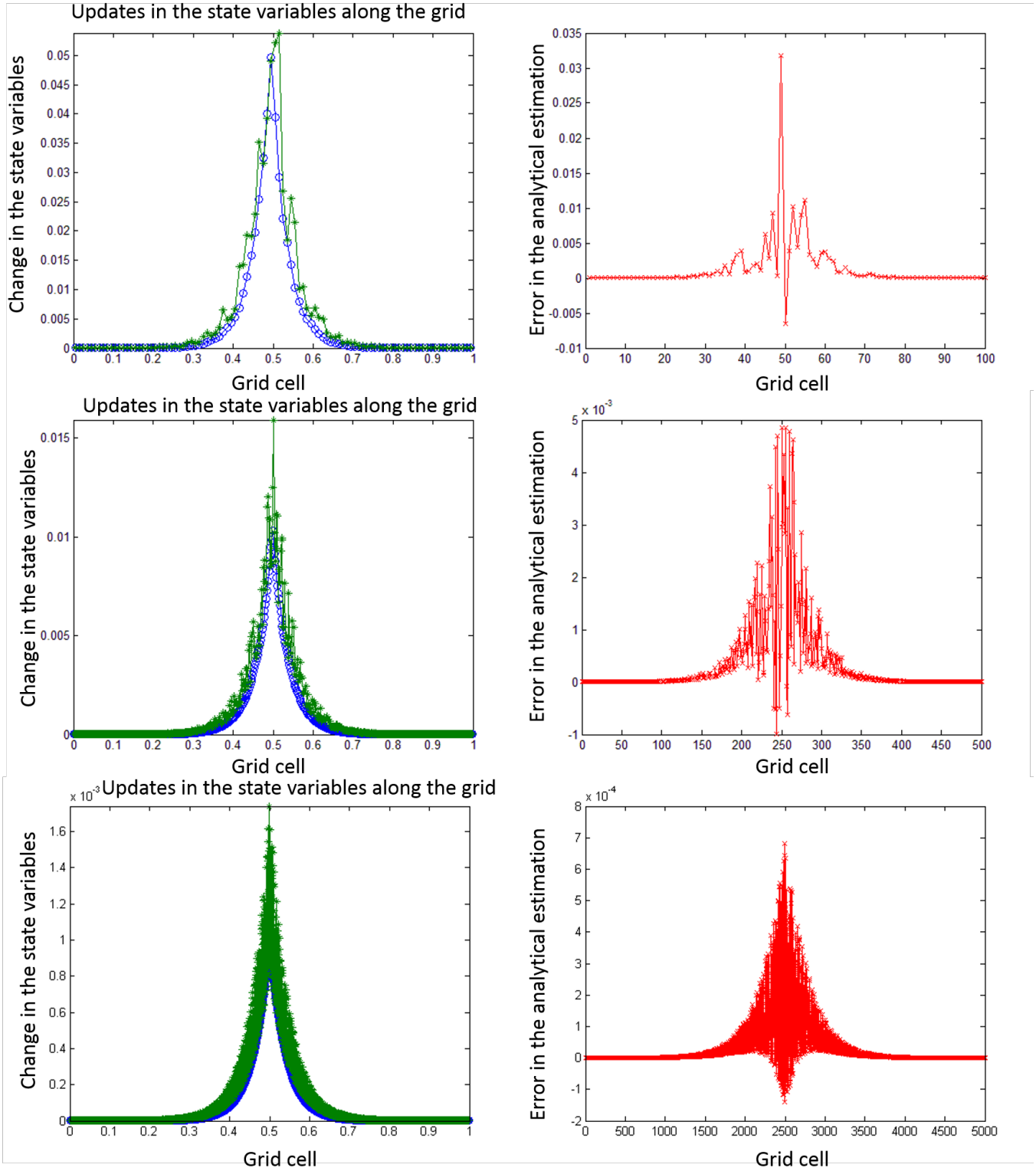

Figure 2.8: Studying the change in absolute error in the estimation of Newton update with resolution of the spatial discretization.

counterpart the error is in the order of 10^{-4}.

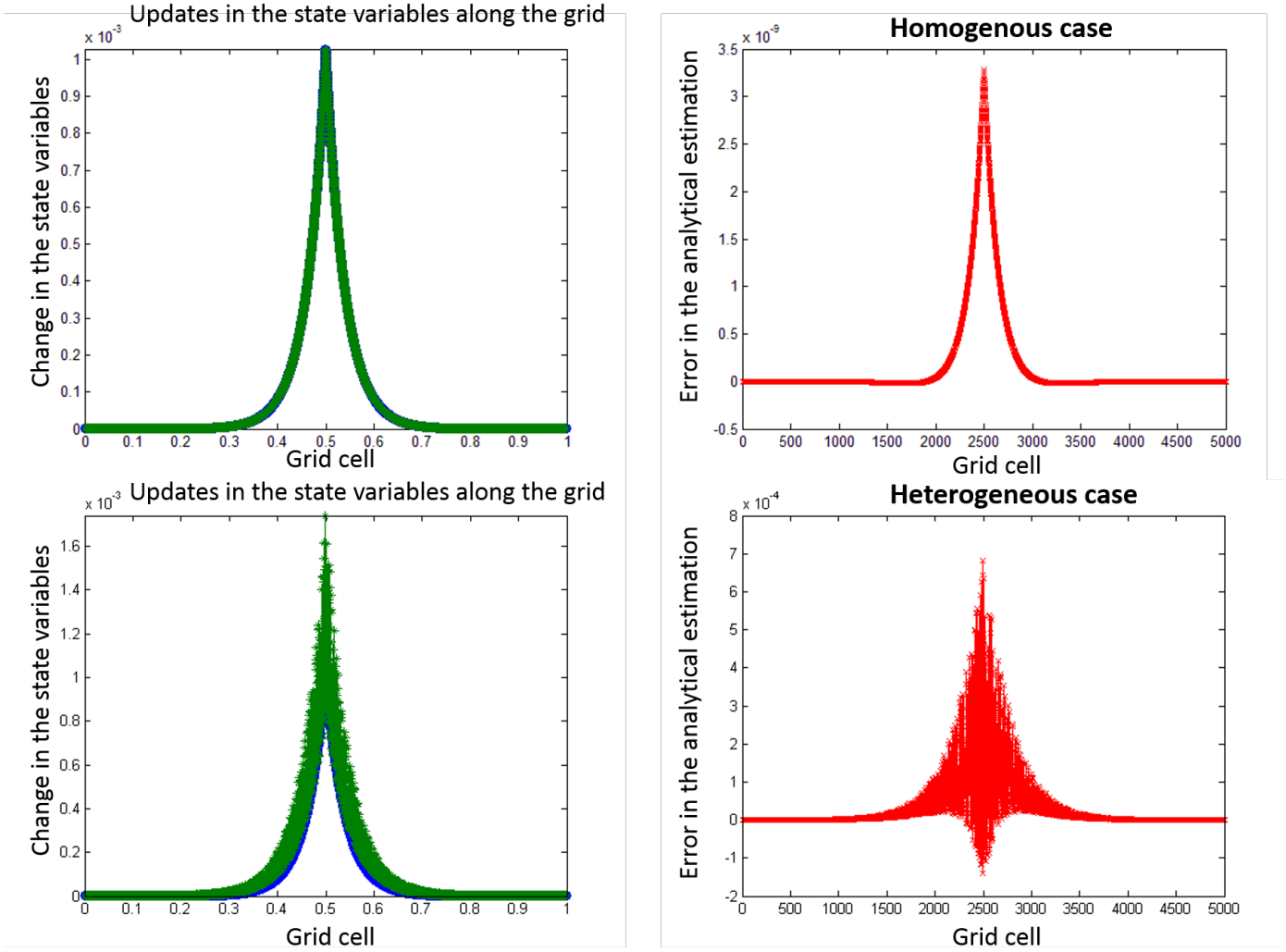

Figure 2.9: Error in the homogeneous case compared to its counterpart heterogeneous problem.

This concludes the spatiotemporal change estimation for the flow problem. We derived the analytical expressions for the calculation of the instantaneous change in the flow variables for a particular time step, Δt. The analytical estimate can be correlated to the numerical simulation with certain algebraic simplifications and a link is developed between the infinite dimensional Newton to the finite dimensional Newton's method. Then after, it is shown that the estimate is conservative and sharp and the support of the numerical update is contained in the support of the estimate. For homogeneous problem the error is in the order of 10^{-9}

and the support of the analytical estimate exactly matches support of the numerical solution. The error in the estimation decreases with the increase in the resolution of discretization. The error increases with the increase in degree of heterogeneity as shown in Figure 2.10. This is due to the heterogeneity term neglected in the derivation of the analytical estimate. To decrease this error and obtain close and conservative estimates, a new formula must be derived which takes in consideration the heterogeneity in the physics. This information holds wide range of applications which will be discussed in the following chapters.

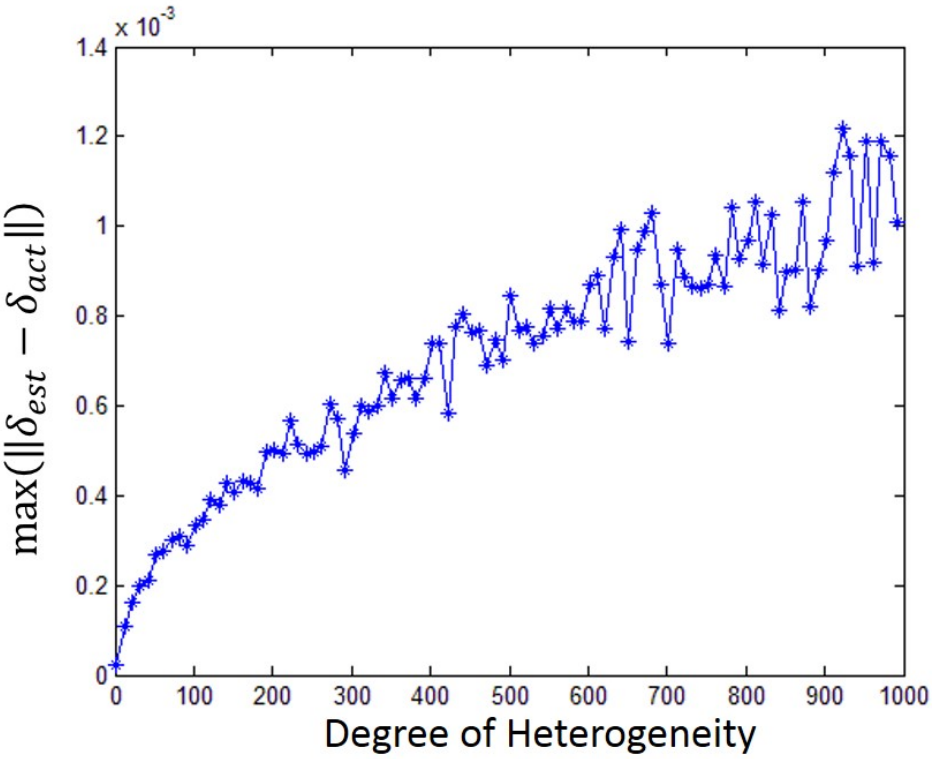

Figure 2.10: Absolute error in estimation as a function of increasing degree of heterogeneity.

CHAPTER 3

THE TRANSPORT EQUATION

Flow equation being an elliptic equation exhibits a global support. Unlike pressure, the transport equation behaves in a hyperbolic wave manner. The locality in the support of the instantaneous change is governed by the nonlinear wave dynamics which forces the transport variables to evolve in a strictly local fashion. This property helps preserve the locality over a timescale that is on the order of years. It's effortless to hypothesize that determining the support of the spatiotemporal change in the transport variable is critical to understand the behavior of a coupled flow transport system and further on to apply this knowledge to complicated simulation problems including unconventional reservoirs.

The following sections deal with the mathematical derivations of the infinite dimensional Newton iteration and the analytical solution to the estimate of unknown Newton update.

3.1 Newton's iterations

The canonical form of the decoupled transport equation is given by,

$$\mathcal{R}_{\mathcal{T}}(s) = \frac{\partial}{\partial t} a(s) - \nabla \left[\mathbf{f}(s)\right] + w(\vec{x}, t) = 0 \tag{3.1.1a}$$

where $\vec{x} \in D \subset \mathbb{R}^3,\ t \geq 0$ and boundary and initial conditions as,

$$\mathbf{f}(s) \cdot \hat{n} = 0 \qquad \mathbf{x} \in \partial D,\ t \geq 0, \tag{3.1.1b}$$

$$s = s^0 \qquad \mathbf{x} \in D,\ t = 0 \tag{3.1.1c}$$

Here, the boundary condition is described in terms of the fractional flow across the boundary,

which can be a constant or zero. Similarly to the flow equation, to search for the solution of Equation 3.1.1a, with auxiliary conditions given by Equation 3.1.1b and 3.1.1c, the first step is deriving the semi-discrete form, maintaining continuity in space. Applying the backward Euler discretization in time to Equation 3.1.1a, we obtain,

$$\begin{cases} \mathcal{R}_{\mathcal{T}}(s^{n+1}) = \mathbf{a}(s^{n+1}) - \mathbf{a}(s^{n}) - \Delta_t \nabla[\mathbf{f}(s^{n+1})] + \Delta_t w(x,t) = 0 & \mathbf{x} \in D \subset \mathbb{R}^3,\ t \geq 0, \\ \mathbf{f}\left(s^{n+1}\right).\hat{n} & \mathbf{x} \in \partial D,\ t \geq 0, \\ s^{n=0} = s_{init}\left(x\right) & \mathbf{x} \in D \subset \mathbb{R}^3,\ t = 0 \end{cases} \tag{3.1.2}$$

$n = 0, 1, 2 \ldots$

To obtain the Newton update a sequence of functions is generated,

$$\left[s^{n+1}\right]^{\nu+1} - \left[s^{n+1}\right]^{\nu} = \delta^{\nu+1};\ \nu = 0, 1, 2 \ldots,\ n = 0, 1, 2 \ldots$$

where $\delta^{\nu+1}$ is the unknown Newton update which can be obtained by solving a linear differential equation. Henceforth, $[s^{n+1}]^{\nu}$ will be represented by s^{ν} to make the notations simplified.

The next step towards the solution is to derive the Frećhet derivative of the functional given by Equation 3.1.2. This will result in a linear differential operator equation which is linear with respect to the instantaneous change in the saturation variables, $\delta^{\nu+1}$. We will follow the same procedure as in the derivation of the derivative of the functional given by Equation 2.1.2.

We will begin with writing the perturbed transport state in the direction of the instantaneous change as,

$$s^{(\nu)} + \epsilon\delta^{(\nu+1)}$$

Subsequently, the residual equation given by Equation 3.1.2 evaluated at the perturbed state

become,

$$\mathcal{R}_{\mathcal{T}}(s^{\nu}+\epsilon\delta^{\nu+1}) = \mathbf{a}([s^{n}]^{\nu}) - \mathbf{a}(s^{\nu}+\epsilon\delta^{\nu+1}) - \Delta_t\nabla\left[\mathbf{f}(s^{\nu}+\epsilon\delta^{\nu+1})\right] + \Delta_t w(s^{\nu}+\epsilon\delta^{\nu+1}) = 0 \quad (3.1.3)$$

Frećhet derivative obtained by,

$$\mathcal{R}'_{\mathcal{T}}\left(s^{\nu}\right)\delta^{\nu+1} = \lim_{\epsilon\to 0}\frac{\mathcal{R}\left(s^{\nu}+\epsilon\delta^{\nu+1}\right)-\mathcal{R}\left(s^{\nu}\right)}{\epsilon} \quad (3.1.4)$$

the result is given by,

$$\mathcal{R}'_{\mathcal{T}}\left(s^{\nu}\right)\delta^{\nu+1} = \left[a'\left(s^{\nu}\right)+\Delta_t w'\left(s^{\nu}\right)\right]\delta^{\nu+1} + \Delta_t\nabla\left(\mathbf{f}'\left(s^{\nu}\right)\delta^{\nu+1}\right), \quad (3.1.5)$$

where, $\nu = 0, 1, \ldots$. In the above equation, ∇ represents the gradient operator. Equation 3.1.5 is the *quasilinear* differential equation with respect to the unknown Newton update. We can further reduce this equation by making proper substitutions, but is not as straight forward as the flow problem. To further simplify the above equation, we need to understand the underlying physical properties. **f'**, being a vector, cannot be divided throughout the equation to isolate the unknown Newton update, $\delta^{\nu+1}$.

One of our strategy is to treat each vectorial component separately and derive different equations depending on the number of dimensions. After expanding and rearranging Equation 3.1.6, the general equation is given by,

$$\mathcal{R}'_{\mathcal{T}}\left(s^{\nu}\right)\delta^{\nu+1} = \Delta_t\mathbf{f}'\left(s^{\nu}\right).\nabla\delta^{\nu+1} + \left[a'\left(s^{\nu}\right)+\Delta_t w'\left(s^{\nu}\right)+\Delta_t\nabla\mathbf{f}'\right]\delta^{\nu+1} \quad (3.1.6)$$

The next step in the derivation is to derive the linearized Newton iteration which can be solved for the unknown update. The infinite dimensional Newton iteration can be formulated now and is given by,

$$\begin{cases} \Delta_t \mathbf{f}'\left(s^{\nu}\right).\nabla\delta^{\nu+1} + \left[a'\left(s^{\nu}\right) + \Delta_t w'\left(s^{\nu}\right) + \Delta_t \nabla \mathbf{f}'\right]\delta^{\nu+1} = \mathcal{R}_{\mathcal{T}}\left(s^{\nu}\right) \quad x \in D \\ \delta^{\nu+1}_{x=\partial D} = 0, \end{cases}, \ \nu = 0, 1, \ldots \tag{3.1.7}$$

Furthermore, we can simplify the problem by introducing constants which results in,

$$\mathcal{R}_{\mathcal{T}}\left(s^{\nu}\right) = \Delta_t \mathbf{f}'\left(s^{\nu}\right).\nabla\delta^{\nu+1} + \left[a'\left(s^{\nu}\right) + \Delta_t w'\left(s^{\nu}\right) + \Delta_t \nabla \mathbf{f}'\right]\delta^{\nu+1} \tag{3.1.8}$$

Equation 3.1.8 must be solved analytically to obtain the update, $\delta^{\nu+1}$. The solution strategy depends on the number of dimensions. For a one-dimensional case, Equation 3.1.8 is reduced further provided,

$$\Delta_t \mathbf{f}' \neq 0$$

We can simplify the Frećhet derivative by introducing an intermediate variable,

$$\hat{\delta} = \Delta_t \mathbf{f}' \delta$$

Equation 3.1.8 becomes,

$$\frac{\partial}{\partial x}\hat{\delta}^{\nu+1} + \frac{\left[a'\left(s^{\nu}\right) + \Delta_t w'\left(s^{\nu}\right) + \Delta_t \nabla \mathbf{f}'\right]}{\Delta_t \mathbf{f}'\left(s^{\nu}\right)}\hat{\delta}^{\nu+1} = \mathcal{R}_{\mathcal{T}}\left(s^{\nu}\right) \tag{3.1.9}$$

Hence, the final reduced equation can be written as,

$$\frac{\partial}{\partial x}\hat{\delta}^{\nu+1} + h\left(x\right)\hat{\delta}^{\nu+1} = \mathcal{R}_{\mathcal{T}}\left(s^{\nu}\right) \tag{3.1.10}$$

or,

$$\frac{\partial}{\partial x}\hat{\delta}^{\nu+1} + h\left(x\right)\hat{\delta}^{\nu+1} = \mathcal{R}\left(x\right) \tag{3.1.11}$$

In the multi-dimensional case the introduction of the new variable is not valid, i.e. $\Delta_t \mathbf{f}'$ is a vector and division by a vector is not defined. Hence, the favorable strategy would be

to separate each dimensional dependent term and writing the equation into a linear partial differential equation form. In the case of three dimensions the final equation can be written in the form,

$$\Delta_t \left[\mathbf{f'}_x \hat{i} + \mathbf{f'}_y \hat{j} + \mathbf{f'}_z \hat{k} \right] . \left[\frac{\partial}{\partial x} \hat{i} + \frac{\partial}{\partial y} \hat{j} + \frac{\partial}{\partial z} \hat{k} \right] \delta^{\nu+1} + \left[a' \left(s^{\nu} \right) + \Delta_t w' \left(s^{\nu} \right) + \Delta_t \nabla \mathbf{f'} \right] \delta^{\nu+1} = \mathcal{R}_{\mathcal{T}} \left(s^{\nu} \right) \quad (3.1.12)$$

Hence, the final equation in three Cartesian dimensions can be written as,

$$\alpha_x \frac{\partial}{\partial x} \delta^{\nu+1} + \alpha_y \frac{\partial}{\partial y} \delta^{\nu+1} + \alpha_z \frac{\partial}{\partial z} \delta^{\nu+1} + \beta \left(x, y, z \right) \delta^{\nu+1} = \mathcal{R} \left(x, y, z \right) \quad (3.1.13)$$

where, $\alpha_x = \Delta_t \mathbf{f'}_x$, $\beta = \left[a' \left(s^{\nu} \right) + \Delta_t w' \left(s^{\nu} \right) + \Delta_t \nabla \mathbf{f'} \right]$ and $\mathcal{R}$ is the spatially varying residual operator.

Equations 3.1.11 and 3.1.13 are the final linearized general Newton iterations, which must be now solved for the unknown update, $\delta^{\nu+1}$.

3.2 Analytical solution

In the previous section, we derived the general Newton iterations for the transport problem in one and three dimensions. Unlike the flow problem, here we do not need to homogenize the variable coefficients. Hence, we will directly seek the solution for these differential equations analytically and establish the connections to the numerical simulation. Now we will deal with the solution of Equations 3.1.11 and 3.1.13.

Figure 3.1 describes the one dimensional transport problem with water injection from the left of the core, fully saturated with oil. The boundaries are at x = 0 and x = 1 with Dirichlet condition. The equation to be solved is an ordinary differential equation with spatially varying coefficient, $h\left(x\right)$ and $\mathcal{R}\left(x\right)$. The one dimensional linear Newton update problem with Dirichlet boundary conditions is given by,

$$\begin{cases} \frac{\partial}{\partial x}\hat{\delta}^{\nu+1} + h\left(x\right)\hat{\delta}^{\nu+1} = \mathcal{R}\left(x\right) \quad x \in D \\ \hat{\delta}^{\nu+1}_{x=\partial D} = 0, \end{cases}, \ \nu = 0, 1, \ldots \tag{3.2.1}$$

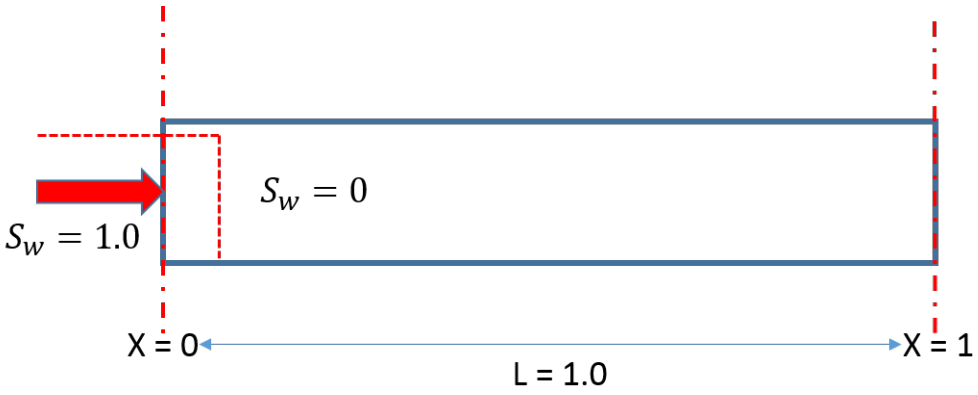

Figure 3.1: One dimensional problem statement with water injection from the left of the core with zero initial water saturation.

Equation 3.2.1 is solved directly and the solution is given by,

$$\delta^{\nu+1} = -e^{-\int_0^x h(y)dy} \int_0^x e^{\int_0^x h(y)dy}\, \mathcal{R}(u)du \tag{3.2.2}$$

3.3 Connection to numerical simulation

In the previous sections we obtained the analytical solutions for the unknown Newton updates for the transport problem. Being integral equations, its unrealistic to try and establish the connections to the numerical simulation. For this purpose, algebraic approximations are developed which reduce the continuous integral solution into a discrete summation equation. The first step is to make an assumption on the spatially varying residual. We assume that in one grid cell the residual value is constant and otherwise zero. This is shown in figure reffig:transportResid, where the bump function is the actual residual but is approximated by the step function. The nonzero value spans over one grid block of size Δx_i and hence the integral evaluated over the domain reduces to the product of the value residual in that grid block and the size of the block.

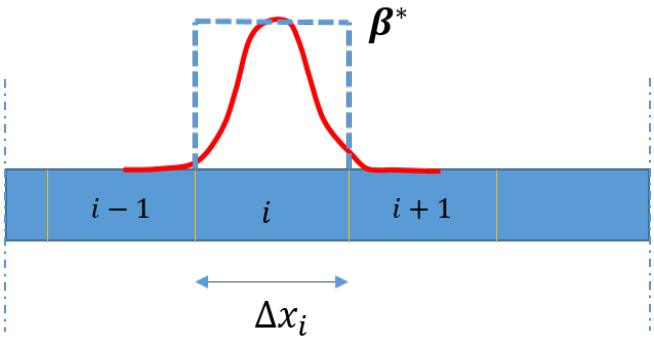

Figure 3.2: Approximation of the nonzero residual in one grid block by a constant step function.

Subsequently, Equation 3.2.2 reduces to

$$\delta^{\nu+1} = -exp\left(-\int_0^x h(y)dy\right)\ exp\left(\int_0^{x_i} h(y)dy\right)\ \mathcal{R}_i\Delta x_i. \tag{3.3.1}$$

The only integral terms remaining are the exponent terms which span over the grid blocks. Spatial integration can be written in a discrete form by introducing summation operator which results in a conservative estimate of the unknown Newton update. The integral term can be rewritten as

$$\int_0^x h(y)dy = \sum_{i=1}^{i(x)-1} h[i]\ Dx[i],$$

where $h[i]$ is the value of the coefficient evaluated in the ith grid cell and $Dx[i]$ is the size of that particular grid cell.

Finally, the discrete summation equation can be written as

$$\delta^{\nu+1} = -exp\left(\sum_{i=1}^{i(x)-1} h[i]\ Dx[i]\right)\ exp\left(\sum_{i=1}^{i(x_i)-1} h[i]\ Dx[i]\right)\ \mathcal{R}_i\Delta x_i, \tag{3.3.2}$$

where $\delta^{\nu+1}$ is derived from the analytical formulation and applied onto the discrete mesh. As the derivation comes from the analytical equation, it is independent of the underlying discretization and can be projected onto any spatial discrete domain.

3.4 Results and conclusions

The aim here was to formulate an analytic method which gives us precisely where is the instantaneous change taking place in the state variables in the spatial domain irrespective of the underlying discretization. The results presented in this section deal with the decoupled transport variables for a one dimensional reservoir. Water injection, $S_w = 1.0$, is from the left of the core with an initial water saturation of 0.0.

Application of the analytical formulas result in the green curve in Figure 3.3. This is the estimated update in the saturation variable for a Newton iteration with a physical time step, Δt. The numerical update is represented by the blue curve (with circle markers), which results from the numerical solution of the nonlinear governing equation. As can be observed, the analytical estimate is a smooth curve in the case of transport, unlike in the case of flow. This is mainly due to the absence of any homogenization process in the derivation towards the solution of the infinite dimensional Newton iteration for saturation.

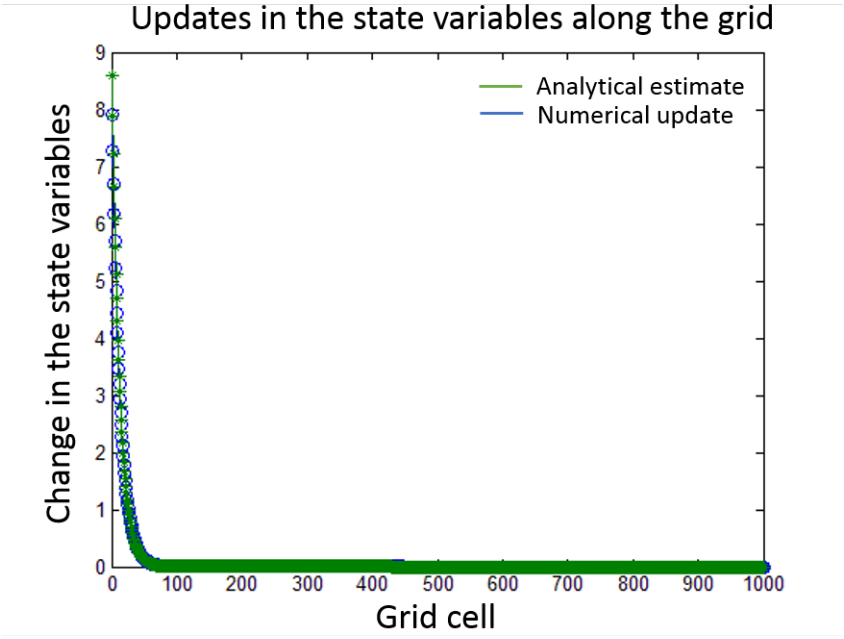

Figure 3.3: Analytical estimate vs. numerical update in the transport state variables for a water injection problem for one Newton iteration. Water injection is from the left of the core.

Figure 3.3 shows the saturation update curve for the first iteration with the first grid cell

acting an a nonzero residual source. Hence, the curve has a monotonic decline as we move towards the other end of the core.

After the first iteration, the scenario complicates due to the introduction of multiple nonzero residual sources caused by the traveling saturation front. Figure 3.4 gives one such scenario of an update at an iteration, $\nu > 1$. As can be seen in this case, analytical solution predicts the update behavior closely and the estimate obtained is still conservative.

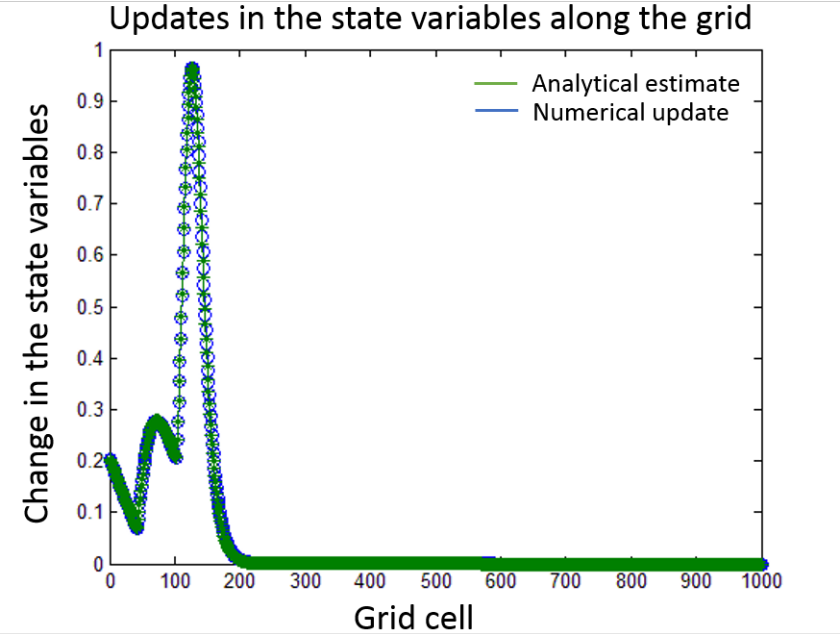

Figure 3.4: Analytical estimate vs. numerical update in the transport state variables for multiple nonzero residual sources in one dimension.

Similar to flow, we present the figure showing the spatiotemporal support for analytical and numerical update. In Figure 3.5 the cells which show a nonzero Newton update for that iteration is given the value 1.0, while the cells which undergo no change in the saturation are given the value 0. As can be observed from the figure, the support of the analytical update matches the support derived from the numerical simulation.

A very important aspect to be considered here is the connection between the discrete Newton's method to the infinite dimension Newton's iteration. If $\hat{\delta}$ is the analytical solution to the governing transport equation and δ^* is the numerical solution obtained from discrete

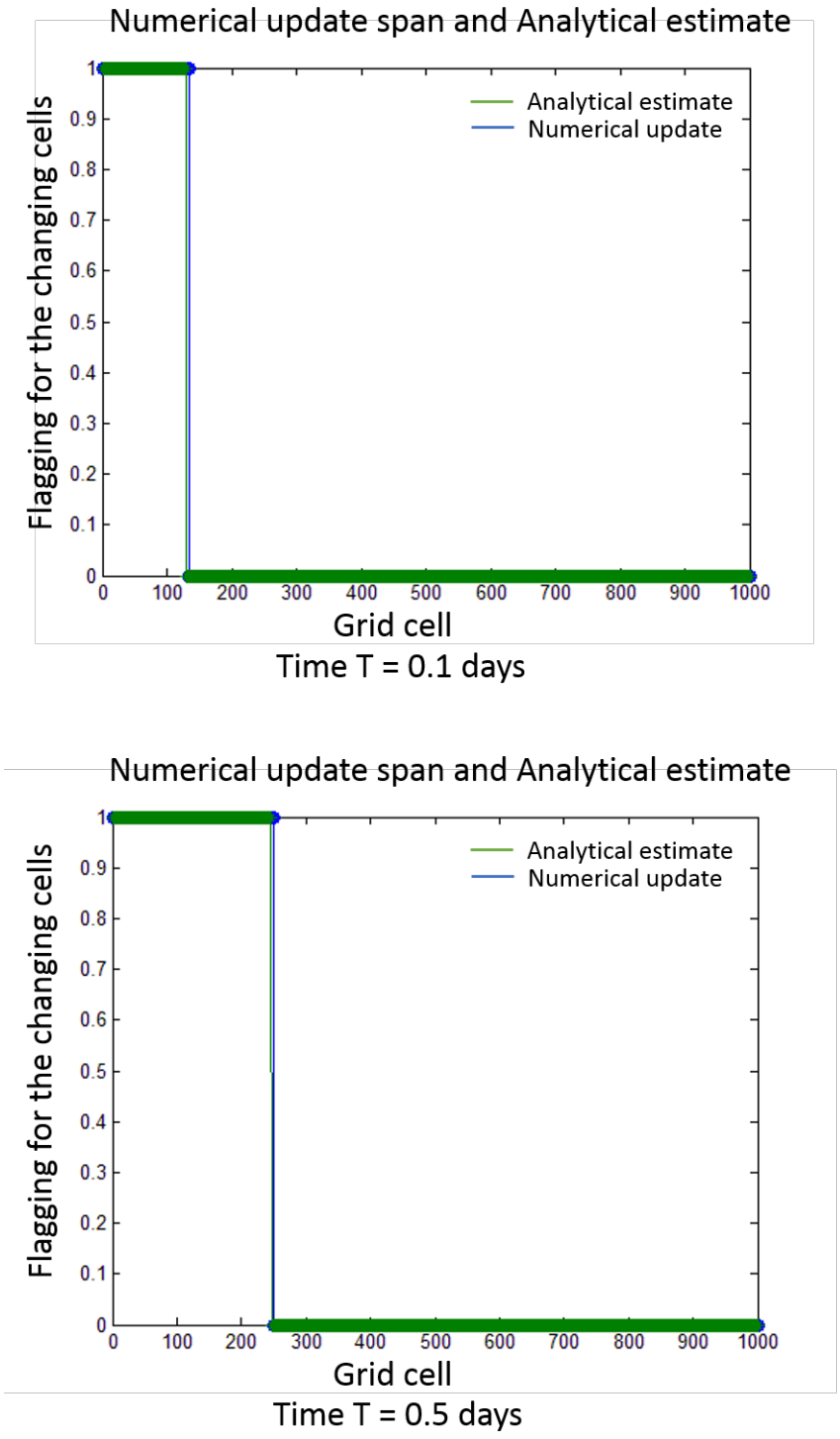

Figure 3.5: Spatiotemporal support of the analytical estimate and the numerical update for a one dimensional transport problem.

Newton's method then,

$$\hat{\delta} = \delta^* + \epsilon$$

Where, ϵ is the discretization error in the spatial domain. The theory we are following in this thesis is to derive an estimate, which is always an upper bound to the analytical solution given by $\hat{\delta}$. Instead of the discrete Newton's method, infinite dimensional Newton's iteration is used to linearize the equation and solve for the update. Will the estimate generated through this method always be an upper bound to the discrete Newton's method? Specifically, for a very coarse grid, will it still produce a conservative upper bound estimate?

Theoretically, it is very difficult to answer this question because of the inability to determine the magnitude of discretization error for different grid sizes. To answer this question for our specific cases, we present the simulation results of the same problem with different discretization resolution. Figure 3.6 shows the comparison between grid size of 100, 500 and 5000 cells. As it can be observed, the error increases as the grid coarsens but the estimate is still quite conservative to the discrete Newton's solution.

This concludes the derivation of estimates for spatiotemporal change in the transport variables. In one dimension the estimates are very local and an upper-bound to the discrete update. For the multiple dimensional cases, the equation is very difficult to solve because of the variable coefficients in space. Alternative solution strategies will be explored in the near future. Being a hyperbolic Partial Differential Equation, the evolution of state is very local. This property can be exploited to develop certain solvers that can be adapted to the underlying physics to increase the computational efficiency.

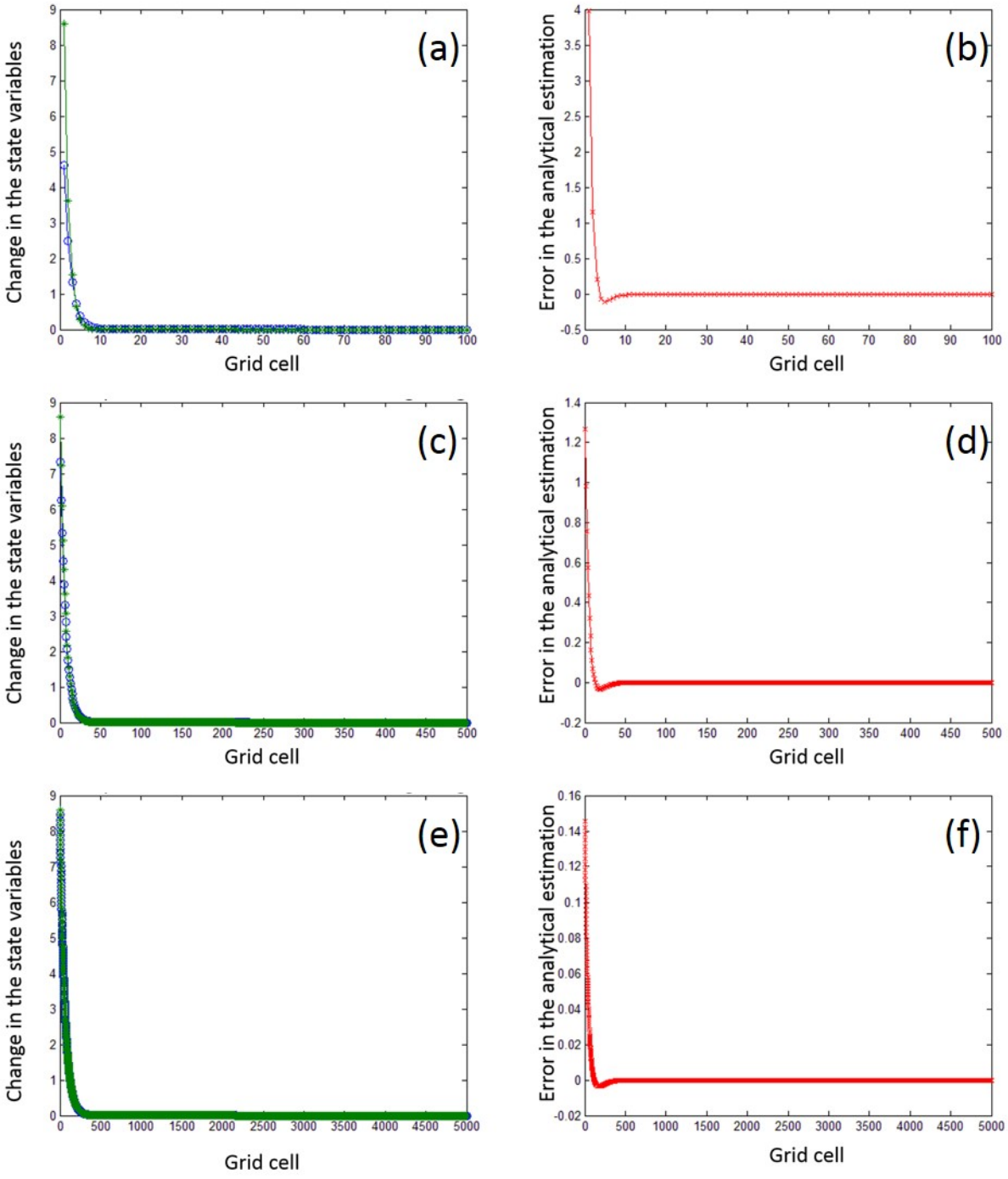

Figure 3.6: Comparison between the error in estimation of the analytical update for different discretization resolutions. (a),(c) and (e) show the analytical and numerical solutions to the transport problem. The corresponding error in estimation is given by (b),(d) and (f). As observed, finer the resolution, smaller is the error.

CHAPTER 4

APPLICATION: NONLINEAR SOLVER

Analytical equations are derived for flow and transport systems which give us a conservative yet sharp estimate of the instantaneous change in the state variables. This information has far reaching applications. Consider the scenario described by figure 4.1, which shows the iteration graph of one dimensional Buckley-Leverett problem. The thick red lines are the converged state values for some initial time, t_1, and the final time, t_2. The lines enclosed between these two lines are Newton iterates which eventually converge to the final state. As evident from the figure, for any Newton like method, the least number of iterations taken for the state to converge for a time-step size of Δt is equal to the number of blue lines.

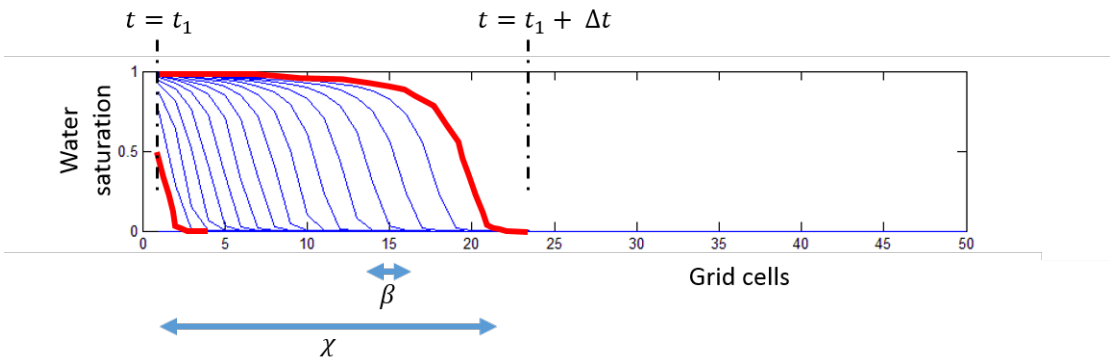

Figure 4.1: Iteration graph for one dimensional Buckley-Leverett problem. χ is the span of the time step and β is the span of each iterate.

This can be roughly summarized as *upperbound* on the convergence rate for the particular problem. Our aim here is to expedite the iterative process. Out of many possible ways, the two most promising are, either to adopt non-Newton like methods which might produce the solution in one step or expedite each iteration which will eventually lead to a faster iterative process. The latter approach will be taken in the thesis, and we will discuss

strategies to expedite the iterations. Figure 4.2 shows 4 Newton iterations for the pressure solve, wherein the nonzero Newton updates are given by the colored surface. The purpose of this figure is to figuratively describe the Newton's process for physical problems. In most of the cases, the Newton update is very local, but due to the inability to detect the nonzero update cells, we need to solve the full linear system in order to obtain the solution.

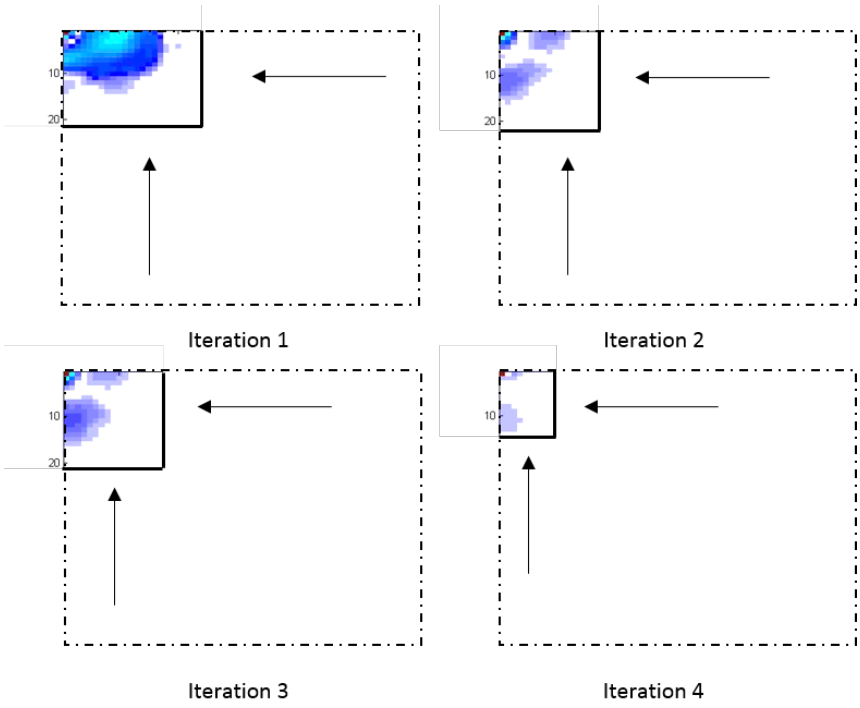

Figure 4.2: Nonzero Newton updates for 4 pressure iterations. Figures shows the reduced Jacobian size to exactly match the nonzero updates.

In that case, to obtain a few nonzero Newton updates, we are solving the entire system, which produces zero updates in the rest of the domain.

What if there was an exact method which provides you with the information on which cells are going to experience a nonzero Newton update a *priori*? Having this information will let us adapt our computational kernel to exactly modify the size of the linear system to match the nonzero Newton updates. We are already equipped with an analytical exact method which gives an estimate of support of the instantaneous change in the state variables, which is described in the previous chapters. Revisiting figure 4.2, we can show that the size of the linear system can be reduced from the entire domain to exactly match the size of the

black square encompassing the spatiotemporal support of the nonzero change. Reduced linear system size reflects directly on the size of the Jacobian and the size of the matrix reduces to the size of the black square in Figure 4.2. The most computationally expensive step is the inversion step required by the Newton's method. The two critical parameters which affect the computational time are the sparsity pattern and size of the Jacobian matrix. In a fixed physical setting, the reduction in the size of the Jacobian does not alter the sparsity pattern, because the physics is not altered. Consequently, the smaller the matrix size, the cheaper is the linear solve.

4.1 Localization

As discussed earlier in the chapters, modeling of fluid flow in porous media deals with the solution of governing equations which involve the coupling between flow and transport. These equations are highly complex and nonlinear with respect to the state variables which vary with space and time. To solve these equations numerically, Newton's method is used, which is a type of local single point iteration method. The intermediate step in this method is linearization of the governing equations and performing a linear solve which includes inversion of the Jacobian matrix. The inverse of the Jacobian multiplied with the Residual vector gives the Newton update.

The property of Newton update we will exploit in this thesis is the locality. Locality in the physics of a problem is reflected in the update vector. The more locality present in the governing equations, the more local is the update in the state variables. This is well presented in Figure 4.2, where the pressure update is nonzero at places which show a local change in physics. The concept here is to perform computations only at the places where there is an instantaneous change in the state.

This algorithm is a three step paradigm - Detect, Adapt and Solve. The detection step includes the estimation of the spatiotemporal change in the state variables and translation of the analytical result in the form of numerical discrete solution. After we have the information of where exactly the change is happening in the domain, we can adapt the size of the problem

to exactly match the grid cells showing a nonzero instantaneous update. Detection and adaptation are shown in Figure 4.3, where the pressure update distribution shows the sparse Newton update, and the detection gives us the red rectangular area. The cells which will experience a change in that iteration are flagged and are the only ones that need to be solved.

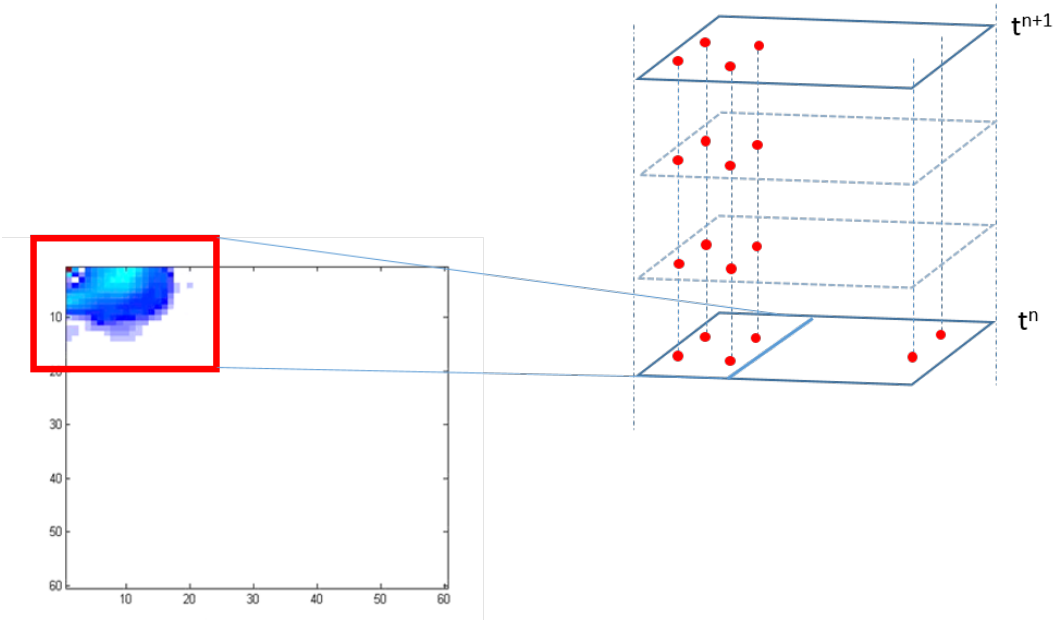

Figure 4.3: Flagging the cells which show a nonzero spatiotemporal change and adapting the computational kernel to the underlying physics.

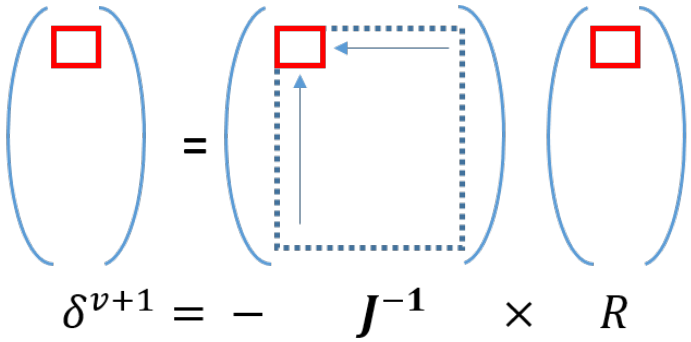

Figure 4.4: Localization: reducing the size of the linear system to exactly match the underlying spatiotemporal change in the state.

Figure 4.4 shows the third step which involves the solution of the reduced system of equations, i.e. equations of those grid cells which show a nonzero update. The reduced

size of the linear system is given by the red square. This is the case where the subdomains to be solved are connected. In the case of disjoint nonzero residual sources which form localized groups, there are multiple strategies to perform the linear solve. First strategy is to transform the disjoint problem into a single domain problem. This is possible in the case of localization because the different subdomains do not interact with each other. Figure 4.5 shows two subdomains which are fused into a single dense block of nonzero updates. This reduced block can be solved using any sequential linear solver.

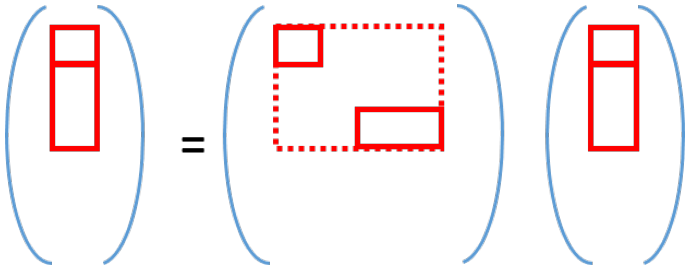

Figure 4.5: Fusing two disjoint subdomains into one dense block and solving it sequentially.

Another strategy which is more attractive is to keep the subdomains distinct and solving two systems separately. Figure 4.6 shows one such scenario where the disjoint subdomains are formed due to multiple nonzero residual sources. Due to the fact that the subdomains are independent of the state variables of the other domains, these distinct systems can be solved in parallel, resulting in an increase in the computational efficiency.

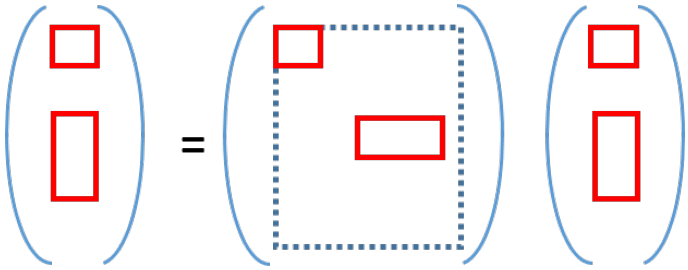

Figure 4.6: Multiple disjoint subdomains can be solved independent of the other in a parallel linear solver.

In a broad sense, the localized nonlinear Newton solver is given by Algorithm 1 where N is the total number of grid cells being simulated and the subscripts g and l stand for global

and local values respectively.

Algorithm 1: Localization with embedded sptiotemporal estimation

Data: $[U^{n+1}]^{\nu} \rightarrow$ state at the previous iterate

input : $\mathcal{R}_g\left(U^{n+1}; U^n, \Delta t\right)$

output: $[U^{n+1}]^{\nu+1} \rightarrow$ updated state for the iterate $\nu + 1$

while *OUTiter* $<$ *MAXITER and* $||\mathcal{R}_g\left(U^{n+1}; U^n, \Delta t\right)|| >$ *TOL* **do**

  for $i \leftarrow 0$ **to** N **do**

    supp$(\hat{\delta})$ from the analytical formulas derived for the spatiotemporal change ;

  end

  Activeset $l \leftarrow i$ if $\hat{\delta}_i > 0$;

  while *INiter* $<$ *MAXITER and* $||\mathcal{R}_l\left(U^{n+1}; U^n, \Delta t\right)|| >$ *TOL* **do**

    $\delta_l \leftarrow -J_l\left({U_l}^{n+1}; {U_l}^n, \Delta t\right)^{-1} \mathcal{R}_l\left({U_l}^{n+1}; {U_l}^n, \Delta t\right)$;

    for $j \leftarrow 0$ **to** l **do**

      if U_j *is a saturation variable* **then**

        $U_j \leftarrow$ UPDATE SAFEGUARD METHOD (U_j, δ_j)

      end

    end

    INiter $\leftarrow$ *INiter* $+1$;

  end

  OUTiter $\leftarrow$ *OUTiter* $+1$;

end

The first step is to perform the analytical-numerical correlation to compute the support of the spatiotemporal change in the state variables. Following this, we have to flag or delineate the cells which are predicted to show a nonzero update for that iteration and then reduce the linear system to be solved. The actual computations are performed only locally on the subdomains generated by the second step. The update step is just adding the solution to the old state, and any safeguard can be used in this place. In this thesis, we

limit ourselves to the use of Modified Appleyard safeguard. The spatiotemporal change is computed at each iteration level for the global system of equations, thus making the solver compute the instantaneous changes in the physics. This results in a dynamically adaptive nonlinear Newton solver.

In later sections we will discuss the results for multirate solver with localization, used to solve decoupled pressure and saturation systems.

4.2 One dimensional transport problem

Transport variables evolve with a hyperbolic wave nature. As discussed already, the more the locality, more the sparsity in the Newton update and this reflects to the fact that a whole lot of computational time goes into inverting a matrix which results in only a few nonzero entries. Applying the above algorithm to similar transport problems, we present the results for one dimensional cases with a certain degree of locality in the underlying physics.

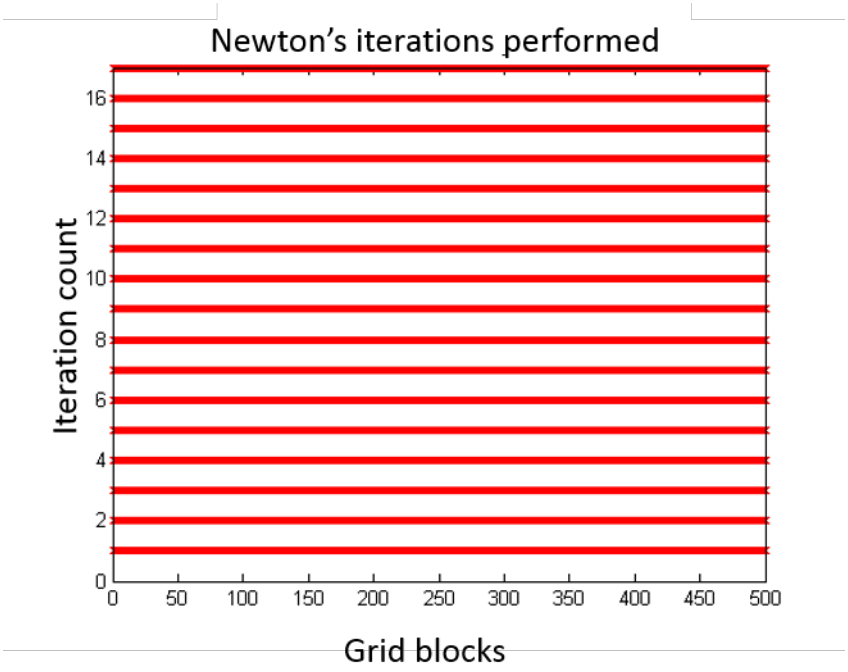

Figure 4.7: Size of the linear system solved at every Newton iteration for a transport problem with a certain physical time step, Δt.

The comparison is done between the traditional Newton's iteration with modified

Appleyard safe update. This would force the solver to consider a linear system of a size equivalent to the size of the domain. On the other hand, we consider the localization algorithm which reduces the size of the linear system to exactly match the grid cells showing a nonzero instantaneous change in the state variable.

Figure 4.7 shows a Newton iteration graph where each red cross indicates the inclusion of that particular grid cell, given on the x-axis, in the Newton iteration given by count on the y-axis. Each horizontal line formed by the crosses is the size of the linear system solved at each Newton iteration for the simulation of the transport problem with a physical time step of Δt.

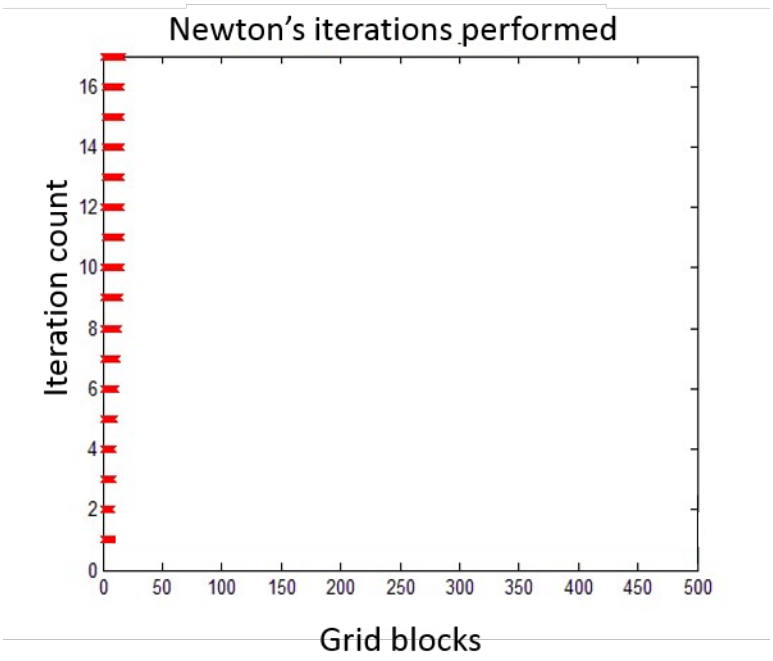

Figure 4.8: Size of the linear system solved at every iteration using spatiotemporal estimation along with localization for the transport problem.

Figure 4.8 shows the Newton iteration graph for the localization solver. Due to the strictly local evolution of the transport component, the resulting spatiotemporal support is compact and limited to a small number of grid cells. Similar to the previous figure, each red line represents the size of the linear system solved at every iteration, which in this case matches the size of the cells that show a nonzero Newton update. In this particular case,

water injection is from the left of the core, which results in one direction wave propagation. In a problem with multiple wells in the region, there will be distinct subdomains of nonzero spatiotemporal change propagating in every direction governed by the underlying heterogeneity.

These results reflect a proof of concept that to solve hyperbolic equations or transport type problems, we do not need to solve the entire grid in order to get the solution. In petroleum systems, simulating compositional properties lead to several governing equations which are hyperbolic or semi-hyperbolic in nature. Using the same concept for the solution of compositional equations may lead to enhanced computational efficiencies, but this topic is of future research interests.

In the above case, the linear system size was reduced from 500 to around 10 grid cells. This means, for transport the number of grid cells undergoing a change is utmost 10 for that particular time step of Δt. The gain in computational efficiency is due to the cheap linear solve and summed up over several iterations, resulting in a total computational save equivalent to all the white space given in Figure 4.8.

4.3 One dimensional flow problem

The second application we will discuss now is the simulation of flow problems. Unlike transport, flow is parabolic/elliptic in nature which results in a more global evolution. In many situations the pressure evolution behaves very locally, such as near wells at early times. Later in the time, flow evolves globally but with different magnitudes with some cells undergoing a significant update, while the rest changing just a bit. To simulate this, we can apply the detection concept discussed in the previous chapters which gives us the information regarding which cells will show an instantaneous change over that time step and then limiting the size of the linear system to the size that exactly matches the number of cells contained inside the nonzero spatiotemporal support. This is called localization. Other strategies will be discussed in the next chapter where the solution strategy is decided by the rate of change of the state variables.

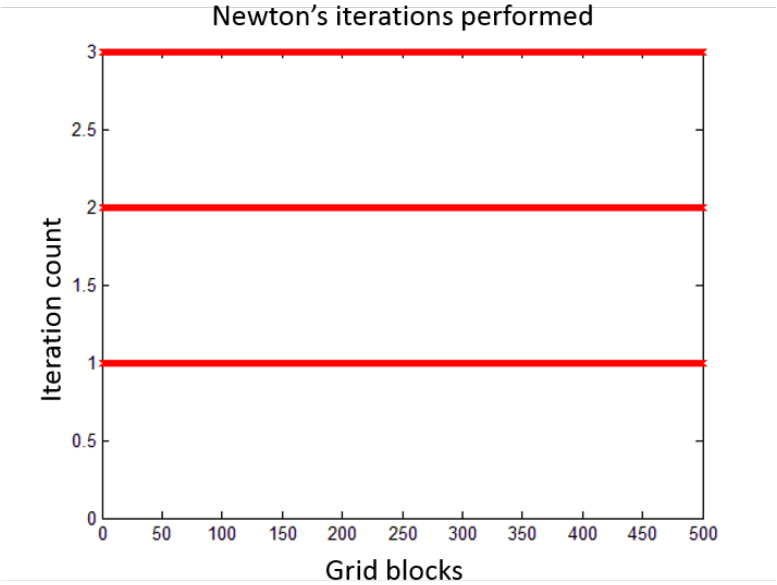

Figure 4.9: Size of the linear system solved at every Newton iteration for a flow problem with a certain physical time step, Δt.

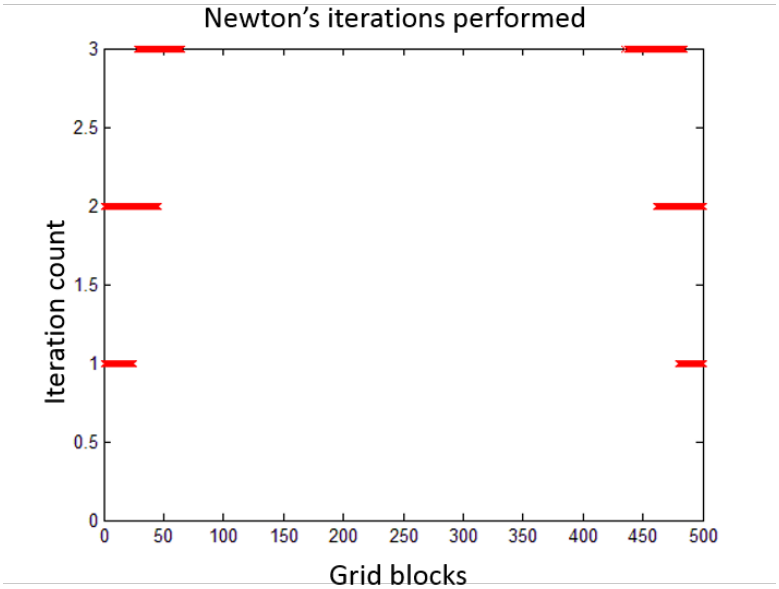

Figure 4.10: Size of the linear system solved at every iteration using spatiotemporal estimation along with localization for the flow problem.

Here we will consider the decoupled flow problem in one dimension, shown in Figure 4.9. For the first case, we will consider one injection and one production well at the two extremes of the reservoir.

Figure 4.9 presents the information of where and when did the Newton iterations take place. Similar to the transport problem, each red cross shows the inclusion of that grid cell in the linear system. Size of the red line gives the size of the linear system to be solved for that iteration. Figure 4.10 shows the reduced system for the localization case. Generally for the case of flow, the state exhibits a global evolution. In the case of localization, the worst case will be equivalent to the traditional Newton's iterations.

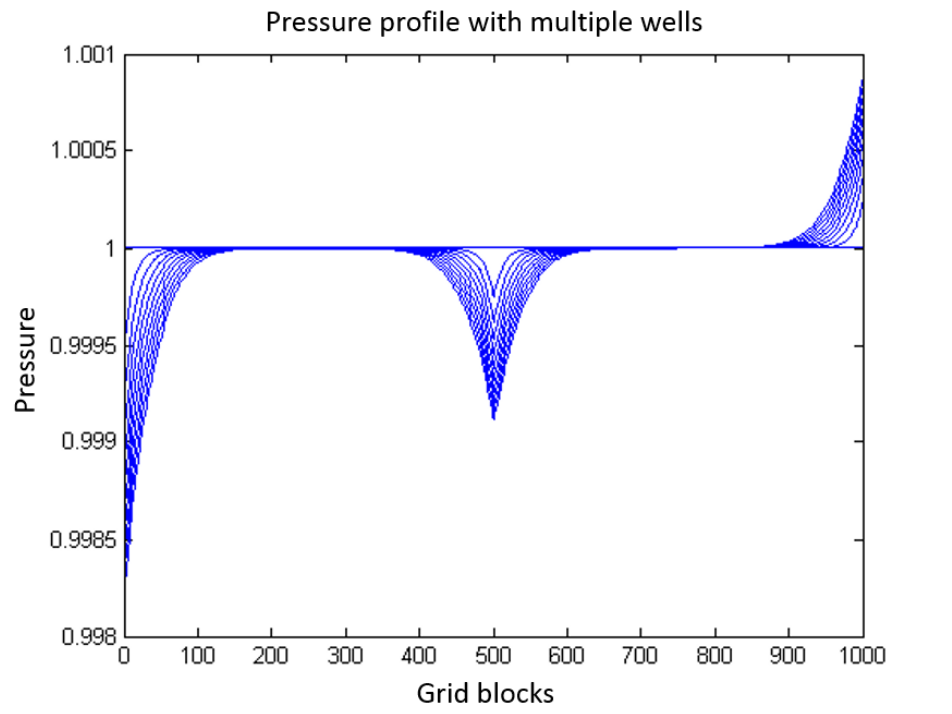

Figure 4.11: Pressure profile for a multiple well case. There is a producer at the center of the grid and at the edge while the injector well on the other extreme of the reservoir.

Let us now consider a case with increasing complexity. In a one dimensional reservoir, we will consider 3 wells which are located at the corners and at the center of the domain. For one particular time step, this simulation takes 3 Newton iterations which are shown in Figure 4.12. The pressure profile for this scenario is given in Figure 4.11. For this case, the

evolution of pressure is considerably local, and the evolution of the spatiotemporal support can be seen the the figure. First, the changes are only around the wells, and as the iterations proceed, the span of nonzero support grows outwards from the wells.

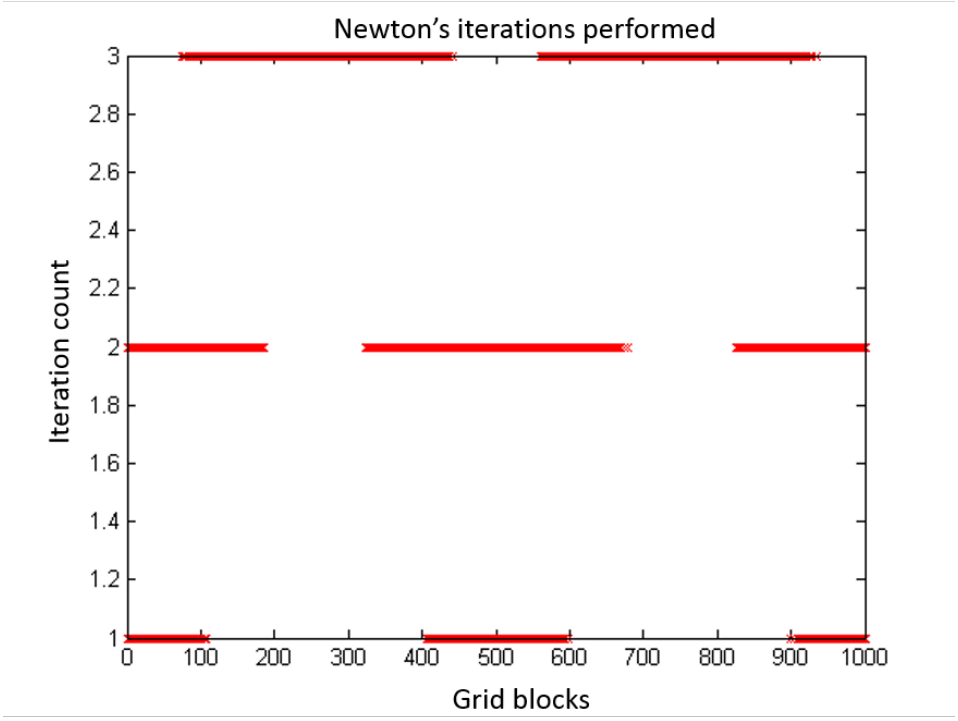

Figure 4.12: Newton iteration graph for the multiple well case. The size of the linear system is the union of the subdomains.

Concluding, we observe that for transport problems, the evolution is strictly local, which results in a small set of cells which show a nonzero update. While in the case of flow, update might be global, but the important thing is that the discrete updates have different magnitudes where the majority possess very insignificant values. This property will be exploited in the next chapter.

CHAPTER 5

DISCUSSION

We derived the analytical formulas for the estimation of the instantaneous spatiotemporal changes in flow and transport and developed connections between the the analytical information to the numerical scheme. The main aim here was to perform calculations only at the places where required. In other words, to determine which cells will show a nonzero Newton update was the first step. With this information, the cells with zero instantaneous change were neglected from the computation thus reducing the size of the linear system which results in a cheaper computation.

Up till now, the derivations were carried out for decoupled flow and transport. Due to the complex equations which need to be solved, for multi-dimensional cases, the solutions to these equations are difficult to obtain. For that purpose semi analytical-numerical solutions will be adopted in the future which have complexity less than $O(N)$.

One of the methods to reduce the algorithmic complexity of detecting the spatiotemporal support is to solve for the radius of nonzero support instead of solving for the update in each grid cell caused due to every nonzero residual. The linear Newton iterations can be directly solved for the radius which produces a nonzero Newton update. Mathematically, instead of solving the equation for $\delta^{\nu+1}$, we can solve for x in the case of $\delta^{\nu+1} > 0$.

There are many advances possible on the application of these analytical formulas derived which concentrate on the nonlinear solver. One important step forward in the future would be to adapt the solver to the rate of change of the state variables. This will be discussed more in the following sections.

5.1 Newton flow

The concept discussed in the previous chapter deals with localization. The domain is flagged into two groups, cells that show a nonzero Newton update and cells that do not. Actual computation is only performed on the cells which are predicted to show an instantaneous update in the state variable. The Newton's method for the reduced system remains the same and is discrete. To further our research in this area we can write the discrete Newton iteration given by,

$$\left[\vec{U}^{n+1}\right]^{\nu+1} - \left[\vec{U}^{n+1}\right]^{\nu} = -\mathbf{J}^{-1}\mathcal{R}\left(U^{n+1}; U^{n}, \Delta t\right)$$

in a continuous form as,

$$\frac{dU^{n+1}}{d\nu} + \mathbf{J}^{-1}\mathcal{R}\left(U^{n+1}; U^{n}, \Delta t\right) = 0 \tag{5.1.1}$$

Discrete Newton's iterations can be summarized as a fixed point iteration strategy using a first order finite difference with unit step size, $\Delta\nu = 1$. We will refer ν as the embedded time step which is completely independent of the simulation time step, Δt, which is fixed for the Newton iteration.

The next step in this research is to extend the localization algorithm to a multirate implementation in the Newton embedded time, independent of the physical time step. Hence, the concept of multirate will be applied on to the solver and not onto the numerical scheme which has been done in the past.

5.2 Multirate solver

Revisiting the solution process of physical processes in the subsurface, we recollect that the Newton's iteration is used to solve the system of equations. We previously showed that the Newton's update is very sparse in cases of highly local physical changes and applied localization to solve this system. Concentrating on the behavior of flow and transport, the latter behaves in a very local manner, owing to its hyperbolic nature. Talking about the

former, at very early times around the wells, pressure evolves in a local manner which in a matter of time changes globally. Global change results in a global update which means the active set will be the entire domain, which will be similar to solving the entire grid with Newton's method. Usually the scenario where there is a global change in the update is given by a hypothetical case described in Figure 5.1. In most of the physical cases, the pressure update is global but small in magnitude except places with high nonzero residual values.

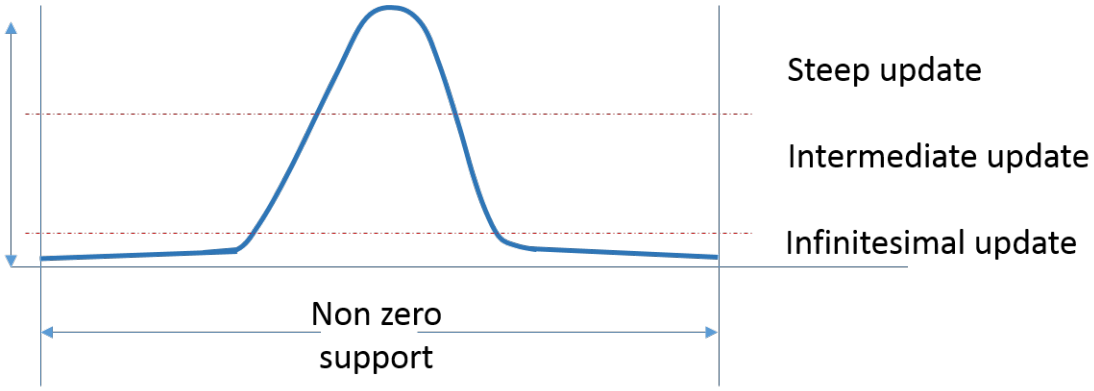

Figure 5.1: Hypothetical pressure update which has a global support but with majority of cells experiencing infinitesimally small update.

In the figure above, the update can be divided into 3 or more partitions. Cells with a steep gradient of change, cells with intermediate rates and the rest are with no or infinitesimally small change. Unlike in localization, where there were two subdomains i.e. the cells that shows a change and those which have zero update, in multirate implementation there will be several subdomains depending on the rates of change of the state variables.

Flagging of these cells is shown in Figure 5.2. Instead of two levels in localization, here there are several number of subdomains depending upon the partition criteria. This strategy makes it more efficient because the cells which do not show a steep gradient might just require 1 iteration to converge to the solution, while those few cells with a bigger instantaneous change can be solved with more iterations. This will result in a bigger save in terms of computations.

For transport problems this strategy will perform efficiently because the interaction between levels of change is not considerable. But for the case of flow, we will need to device

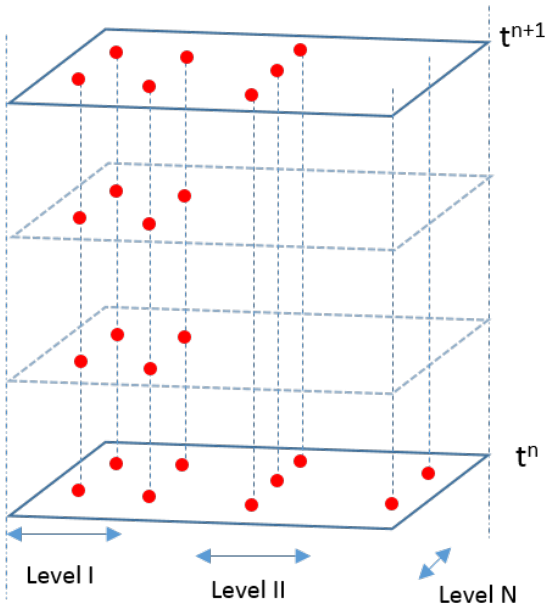

Figure 5.2: Flagging in a multilevel solver, where the subdomains are formed on the criteria of rate of change of state variables.

expensive synchronization strategies which take care of the interaction between different levels. This is because, the variables in one cell are tightly dependent on the state in other grid cells, thus changing the convergence rate for Newton's iterations.

There are many more applications of these ideas, such as development of parallel scalable solvers for implicit simulations, characterization of Newton iteration's convergence rates, exploiting locality and understanding the behavior of flow and transport in unconventional reservoirs, etc. The key lies in deriving closed form analytical estimates of the infinite-dimensional Newton iterations and developing links to the spatial discretization.

BIBLIOGRAPHY

[1] J.E. Aarnes, S. Krogstad, and K.A. Lie. A hierarchical multiscale method for two-phase flow based upon mixed finite elements and nonuniform coarse grids. *Multiscale Modeling & Simulation*, 5(2):337–363, 2006.

[2] M. Ainsworth and J.T. Oden. *A posteriori error estimation in finite element analysis*, volume 37. John Wiley & Sons, 2011.

[3] E.L. Allgower, K. Böhmer, F.A. Potra, and W.C. Rheinboldt. A mesh-independence principle for operator equations and their discretizations. *Society of Industrial Applied Mathematics Journal on Numerical Analysis*, 23(1):160–169, 1986.

[4] K. Aziz and A. Settari. *Petroleum Reservoir Simulation*. Elsevier Applied Science, 1979.

[5] I. Babuvška and W.C. Rheinboldt. Error estimates for adaptive finite element computations. *SIAM Journal on Numerical Analysis*, 15(4):736–754, 1978.

[6] J. Bear. *Dynamics of Fluids in Porous Media*. Dover Civil and Mechanical Engineering. Dover Publications, 1988.

[7] J. Bell, M. Berger, J. Saltzman, and M. Welcome. Three-dimensional adaptive mesh refinement for hyperbolic conservation laws. *SIAM Journal on Scientific Computing*, 15(1):127–138, 1994.

[8] M.J. Berger and P. Colella. Local adaptive mesh refinement for shock hydrodynamics. *Journal of computational Physics*, 82(1):64–84, 1989.

[9] M.J. Berger and R.J. LeVeque. Adaptive mesh refinement using wave-propagation algorithms for hyperbolic systems. *Society of Industrial Applied Mathematics Journal on Numerical Analysis*, 35(6):2298–2316, 1998.

[10] M.J. Berger and R.J. LeVeque. Adaptive mesh refinement using wave-propagation algorithms for hyperbolic systems. *SIAM Journal on Numerical Analysis*, 35(6):2298–2316, 1998.

[11] X.C. Cai, D.E. Keyes, and L. Marcinkowski. Non-linear additive schwarz preconditioners and application in computational fluid dynamics. *International journal for numerical methods in fluids*, 40(12):1463–1470, 2002.

[12] Z. Chen, G. Huan, and Y. Ma. *Computational Methods for Multiphase Flows in Porous Media*. Computational Science and Engineering. Society of Industrial Applied Mathematics, 2006.

[13] A. Datta-Gupta, J. Xie, N. Gupta, M.J. King, and W.J. Lee. Radius of investigation and its generalization to unconventional reservoirs. *Journal of Petroleum Technology*, 63(7):52–55, 2011.

[14] C.N. Dawson, T.F. Russell, and M.F. Wheeler. Some improved error estimates for the modified method of characteristics. *SIAM Journal on Numerical Analysis*, 26(6):1487–1512, 1989.

[15] P. Deuflhard. *Newton methods for nonlinear problems: affine invariance and adaptive algorithms*, volume 35. Springer, 2011.

[16] C. Engstler and C. Lubich. Multirate extrapolation methods for differential equations with different time scales. *Computing*, 58(2):173–185, 1997.

[17] L.C. Evans. Partial differential equations: Graduate studies in mathematics. *American mathematical society*, 2, 1998.

[18] C.W. Gear and D.R. Wells. Multirate linear multistep methods. *BIT Numerical Mathematics*, 24(4):484–502, 1984.

[19] M. Gerritsen and J.V. Lambers. Integration of local–global upscaling and grid adaptivity for simulation of subsurface flow in heterogeneous formations. *Computational Geosciences*, 12(2):193–208, 2008.

[20] M.G. Gerritsen and L.J. Durlofsky. Modeling fluid flow in oil reservoirs. *Annual Reviews in Fluid Mechanics*, 37:211–238, 2005.

[21] R.D. Hornung and J.A. Trangenstein. Adaptive mesh refinement and multilevel iteration for flow in porous media. *Journal of computational Physics*, 136(2):522–545, 1997.

[22] G. Hunter, S. Jeffers, and J.P. Vigier. Causality and locality in modern physics. In *Causality and Locality in Modern Physics*, volume 1, 1998.

[23] F.N. Hwang and X.C. Cai. A parallel nonlinear additive schwarz preconditioned inexact newton algorithm for incompressible navier–stokes equations. *Journal of Computational Physics*, 204(2):666–691, 2005.

[24] P. Jenny, S.H. Lee, and H.A. Tchelepi. Adaptive multiscale finite-volume method for multiphase flow and transport in porous media. *Multiscale Modeling & Simulation*, 3(1):50–64, 2005.

[25] P. Jenny, S.H. Lee, and H.A. Tchelepi. Adaptive fully implicit multi-scale finite-volume method for multi-phase flow and transport in heterogeneous porous media. *Journal of Computational Physics*, 217(2):627–641, 2006.

[26] C.T. Kelley and E.W. Sachs. Mesh independence of newton-like methods for infinite dimensional problems. *Journal of Integral Equations and Applications*, 3(4):549–573, 1991.

[27] F. Kuchuk. Radius of investigation for reserve estimation from pressure transient well tests. In *SPE Middle East Oil and Gas Show and Conference*, 2009.

[28] F. Kwok and H. Tchelepi. Potential-based reduced newton algorithm for nonlinear multiphase flow in porous media. *Journal of Computational Physics*, 227(1):706–727, 2007.

[29] L.W. Lake. *Enhanced Oil Recovery*. Prentice Hall, first edition, 1996.

[30] G. Lodato and W.K.M. Rice. Testing the locality of transport in self-gravitating accretion discs. *Monthly Notices of the Royal Astronomical Society*, 351(2):630–642, 2004.

[31] B.T. Mallison, M.G. Gerritsen, and G. Kreiss. Asynchronous time integration of flux-conservative transport. In *11th European Conference on the Mathematics of Oil Recovery*, 2008.

[32] S. Müller and Y. Stiriba. Fully adaptive multiscale schemes for conservation laws employing locally varying time stepping. *Journal of Scientific Computing*, 30(3):493–531, 2007.

[33] M. Muskat and M.W. Meres. The flow of heterogeneous fluids through porous media. *Physics*, 7(9):346–363, 1936.

[34] H. Mc Namara, G. Bowen, and P.J. Dellar. Locally adaptive timestepping in reservoir simulators. In *12th European Conference on the Mathematics of Oil Recovery*, 2010.

[35] B. Rivière, M.F. Wheeler, and V. Girault. A priori error estimates for finite element methods based on discontinuous approximation spaces for elliptic problems. *SIAM Journal on Numerical Analysis*, 39(3):902–931, 2001.

[36] A. Settari and F.M. Mourits. A coupled reservoir and geomechanical simulation system. *Society of Petroleum Engineers Journal*, 3(3):219–226, 1998.

[37] J.O. Skogestad, E. Keilegavlen, and J.M. Nordbotten. Domain decomposition strategies for nonlinear flow problems in porous media. *Journal of Computational Physics*, 2012.

[38] S. Sun, D. Keyes, and L. Liu. Fully implicit two-phase reservoir simulation with the additive schwarz preconditioned inexact newton method. In *Society of Petroleum Engineers Reservoir Characterisation and Simulation Conference and Exhibition*, 2013.

[39] S. Sun and M.F. Wheeler. A posteriori error estimation and dynamic adaptivity for symmetric discontinuous galerkin approximations of reactive transport problems. *Computer methods in applied mechanics and engineering*, 195(7):632–652, 2006.

[40] J.A. Trangenstein. Multi-scale iterative techniques and adaptive mesh refinement for flow in porous media. *Advances in Water Resources*, 25(8):1175–1213, 2002.

[41] R. Verfürth. A review of a posteriori error estimation. In *and Adaptive Mesh-Refinement Techniques, Wiley & Teubner*. Citeseer, 1996.

[42] M. Wang, A. Ailamaki, and C. Faloutsos. Capturing the spatio-temporal behavior of real traffic data. *Performance Evaluation*, 49(1):147–163, 2002.

[43] M.F. Wheeler. A priori l_2 error estimates for galerkin approximations to parabolic partial differential equations. *SIAM Journal on Numerical Analysis*, 10(4):723–759, 1973.

[44] J. Xie, N. Gupta, M. King, and A. Datta-Gupta. Depth of investigation and depletion behavior in unconventional reservoirs using fast marching methods. In *SPE Europec/EAGE Annual Conference*, 2012.

[45] R.M. Younis. A sharp analytical bound on the spatiotemporal locality in general two-phase flow and transport phenomena. *Procedia Computer Science*, 18:473–480, 2013.

[46] R.M. Younis, H. Tchelepi, and K. Aziz. Adaptively localized continuation-newton method–nonlinear solvers that converge all the time. *Society of Petroleum Engineers Journal*, 15(2):526–544, 2010.

[47] O.C. Zienkiewicz and J.Z. Zhu. Adaptivity and mesh generation. *International Journal for Numerical Methods in Engineering*, 32(4):783–810, 1991.

APPENDIX A

FRÉCHET DERIVATIVE

The definition of a derivative in a very general sense can be given by,

$$\Delta_h f(X_0) = \Lambda(X_0; h).h + \xi(X_0; h) \tag{A.0.1}$$

Here, $\Lambda(X_0; h)$ is a constant (which depends on X_0 and h) and $\xi(X_0; h)$ has the property,

$$\lim_{h \to 0} |\frac{1}{h}||\xi(X_0; h)| = 0$$

The derivative of functionals differ from scalar valued functions because the gradient is computed on a vector quantity. Due to this, the traditional definition of a derivative fails as the division by a vector quantity is not defined. For this purpose, the derivative of a functional is given by Fréchet derivative, which states that an infinitesimal increment in the functional, $\mathcal{F}(X_0)$, evaluated at X_0 is given by $\mathcal{F}(X_0 + s\vec{h})$, where, the increment, s, is in the direction of a vector, $\vec{h}$.

Using Taylor series expansion and some algebraic manipulation, we arrive at the equation when $s \to 0$,

$$\lim_{s \to 0} \frac{\mathcal{F}(X_0 + s\vec{h}) - \mathcal{F}(X_0)}{s} = \vec{h}.\mathcal{F}'(X_0) + \lim_{s \to 0} O(s.\vec{h}) \tag{A.0.2}$$

Here the term $\lim_{s \to 0} O(s.\vec{h}) = 0$ due to the higher orders of s. As it can be observed from the above equation, the remaining terms in the expression are all linear in $\vec{h}$. Hence, this operator results in equation linear in the vector on which the derivative is computed. The final equation is given by,

$$\mathcal{F}'(X_0)\vec{h} = \lim_{s\to 0} \frac{\mathcal{F}(X_0 + s\vec{h}) - \mathcal{F}(X_0)}{s} \tag{A.0.3}$$

Where, $\mathcal{F}'(X_0)$ is the Fréchet derivative evaluated at X_0 and acting on $\vec{h}$.

Note: Fréchet derivative exists only where Gateaux derivative exists and satisfies the condition given by equation (A.0.4), which is a limiting term in the generalized form of a derivative shown in equation (A.0.1)

$$\lim_{||h||\to 0} \frac{||\xi(X_0; \vec{h})||}{||\vec{h}||} = 0 \tag{A.0.4}$$

APPENDIX B

INFINITE DIMENSION NEWTON'S METHOD

The first order discretization in time of the Newton flow Partial Differential Equation (PDE) results in the discrete Newton's iteration, which is used for for solving discrete nonlinear systems. Finer discretization leads to a more exact Newton's method. The finest discretization results in a continuous Newton's iteration which is also knows as *infinite dimensional Newton's method*.

To apply Newton method on discrete systems, we have the discrete Newton's iteration but in order to apply Newton's method directly on to PDEs, the continuous form must be employed. For this purpose, we need the function which is the PDE itself and its derivative. A continuous derivative of a particular group of PDEs, in our case functionals, is given by Fréchet derivative described in APPENDIX A.

Infinite dimension Newton operation on a PDE will result in a quasilinear equation which then can be solved analytically or in a linear solver. The continuous Newton formulation can be given by,

$$\mathcal{F}\left(\left[U^{n+1}\right]^{\nu}\right) = -\mathcal{F}'\left(\left[U^{n+1}\right]^{\nu}\right) \cdot \delta^{\nu+1}; \tag{B.0.5}$$

where, $\mathcal{F}'$ is the Fréchet derivative evaluated at $[U^{n+1}]^{\nu}$ and is acting on $\delta^{\nu+1}$, which is the continuous update or in other words, analytical update to the particular iteration.

Refining the discretization in the Newton flow PDE results in different accuracy Newton iterations. It is studied that with comparable initial guesses all the flavors of Newton's iterations show the convergence behavior on all sufficiently fine discretizations. This is given by the theory of *asymptotic mesh independence*. For further details, please refer to [15].